AN INVESTIGATION OF GROUND-WATER RECHARGE BY INJECTION IN THE PALO ALTO BAYLANDS, CALIFORNIA: HYDRAULIC AND CHEMICAL INTERACTIONS--FINAL REPORT

By Scott N. Hamlin

U.S. GEOLOGICAL SURVEY

Water-Resources Investigations Report 84-4152

Prepared in cooperation with the

SANTA CLARA VALLEY WATER DISTRICT

3010-09

Sacramento, California
April 1985

UNITED STATES DEPARTMENT OF THE INTERIOR

DONALD PAUL HODEL, Secretary

GEOLOGICAL SURVEY

Dallas L. Peck, Director

For additional information
write to:

District Chief
U.S. Geological Survey
Federal Building, Room W-2235
2800 Cottage Way
Sacramento, California 95825

Copies of this report
can be purchased from:
Open-File Services Section
Western Distribution Branch
U.S. Geological Survey
Box 25425, Federal Center
Denver, Colorado 80225
Telephone: (303) 236-7476

CONTENTS

APPENDIXES

ILLUSTRATIONS

TABLES

CONVERSION FACTORS

For readers who prefer to use the International System of Units (SI) rather than inch-pound units, the conversion factors for the terms used in this report are as follows:

Multiply	By	To obtain
acre-ft (acre-feet)	1233	cubic meters
feet	0.3048	meters
ft/d (feet per day)	0.3048	meters per day
ft^2/d (feet squared per day)	0.0929	meters squared per day
gal/min (gallons per minute)	0.00006309	cubic meters per second
inches	25.40	millimeters
°F (degrees Fahrenheit)	°C = 5/9 (°F-32)	°C (degrees Celsius)

Other abbreviations used in this report:

mg/L	milligrams per liter
µg/L	micrograms per liter
mol/L	moles per liter
mmol/L	millimoles per liter
g/L	grams per liter
g/cm^3	grams per cubic centimeter

TRADE NAMES

The use of trade names in this report is for identification purposes only and does not imply endorsement by the U.S. Geological Survey.

AN INVESTIGATION OF GROUND-WATER RECHARGE BY INJECTION IN THE PALO ALTO BAYLANDS, CALIFORNIA: HYDRAULIC AND CHEMICAL INTERACTIONS--FINAL REPORT

By Scott N. Hamlin

ABSTRACT

The U.S. Geological Survey, in cooperation with the Santa Clara Valley Water District, has completed a study of ground-water recharge by injection in the Palo Alto Baylands along San Francisco Bay, California. Selected wells within the Water District's injection-extraction network were monitored to determine hydraulic and chemical interactions affecting well-field operation. The well field was installed to prevent and eliminate saline contamination in the local shallow aquifer system. The primary focus of this report is upon factors that affect injection efficiency, specifically well and aquifer clogging.

Mixing and breakthrough curves for major chemical constituents indicate ion exchange, adsorption, and dissolution reactions. Freshwater breakthrough was detected in water-level data, which reflect fluid-density change as well as head buildup. Of chief interest is the dissolution of calcium carbonate induced by dilution of saline ground water with injected freshwater. Observation of this condition supports hydraulic data, which show an apparent increase in specific capacity, probably the result of improvement in aquifer permeability. Trace elements were removed during passage through the aquifer, but they were otherwise little influenced by injection.

From the standpoint of hydraulic and chemical compatibility, the well field is a viable system for ground-water recharge. Aquifer heterogeneity and operational constraints reduce the efficiency of the system. These problems may be offset by operating the extraction wells as a primary unit in conjunction with periodic operation of the injection wells. In this way, the risk of contamination of adjacent fresh ground water is reduced.

INTRODUCTION

This report concludes an investigation of ground-water recharge by injection in the Palo Alto Baylands, California (fig. 1). A preliminary report (Hamlin, 1983) covers the general topics of geology and hydrology and describes ground-water quality, aquifer characteristics, and hydraulic properties of the system.

The Santa Clara Valley Water District is responsible for the prevention of ground-water-quality degradation in the aquifers used for water supply within the district. In general, ground-water quality is good; however, the shallow baylands aquifer system (less than 150 feet in depth) locally contains saline water. The deep baylands aquifer system (below 150 feet in depth) is protected by a thick confining clay layer and generally produces fresh water of good quality. In some instances, improper well construction and (or) abandonment procedures coupled with heavy pumping have led to localized saline contamination in the deep aquifer. Seawater was assumed to be the source of the contamination in the shallow aquifer system. The Santa Clara Valley Water District installed an injection-extraction well network in an attempt to control the "seawater intrusion" in the Palo Alto Baylands (Brown and Caldwell, 1974).

Chemical analyses of ground water from the shallow baylands aquifer system showed dissolved-solids concentrations much greater than in both seawater and baywater. The shallow baylands aquifer system locally contains an upper (20-foot depth) and a lower (45-foot depth) aquifer separated by a leaky clay layer (fig. 2). Salt concentration, which is greater in the lower than the upper aquifer, apparently has resulted from evaporation within the marsh environment and collection in the aquifer system. The original objective of controlling "seawater intrusion" by constructing a salinity-intrusion barrier (Brown and Caldwell, 1974) may not be attainable with the present system.

The present system is a series of paired injection and extraction wells installed parallel to the bayshore in the marsh (fig. 3). Through coupled freshwater injection and inland ground-water extraction, the Santa Clara Valley Water District hoped to flush the lower aquifer of saline water and form a barrier to prevent further "seawater intrusion." The well network bisects the zone of highest saline concentration in the ground water; rather than flushing and excluding the saline water, the network may induce migration of saline water into the adjacent inland freshwater aquifer.

This report summarizes the hydraulic and chemical effects of injection of treated wastewater from the Santa Clara Valley Water District's treatment plant upon the aquifer system within the injection-extraction well field. Chemical interactions were studied at injection well I9 and hydraulic effects interpreted for injection well I6 (fig. 3). The objective of this analysis is to determine factors that affect injection efficiency, particularly potential clogging mechanisms.

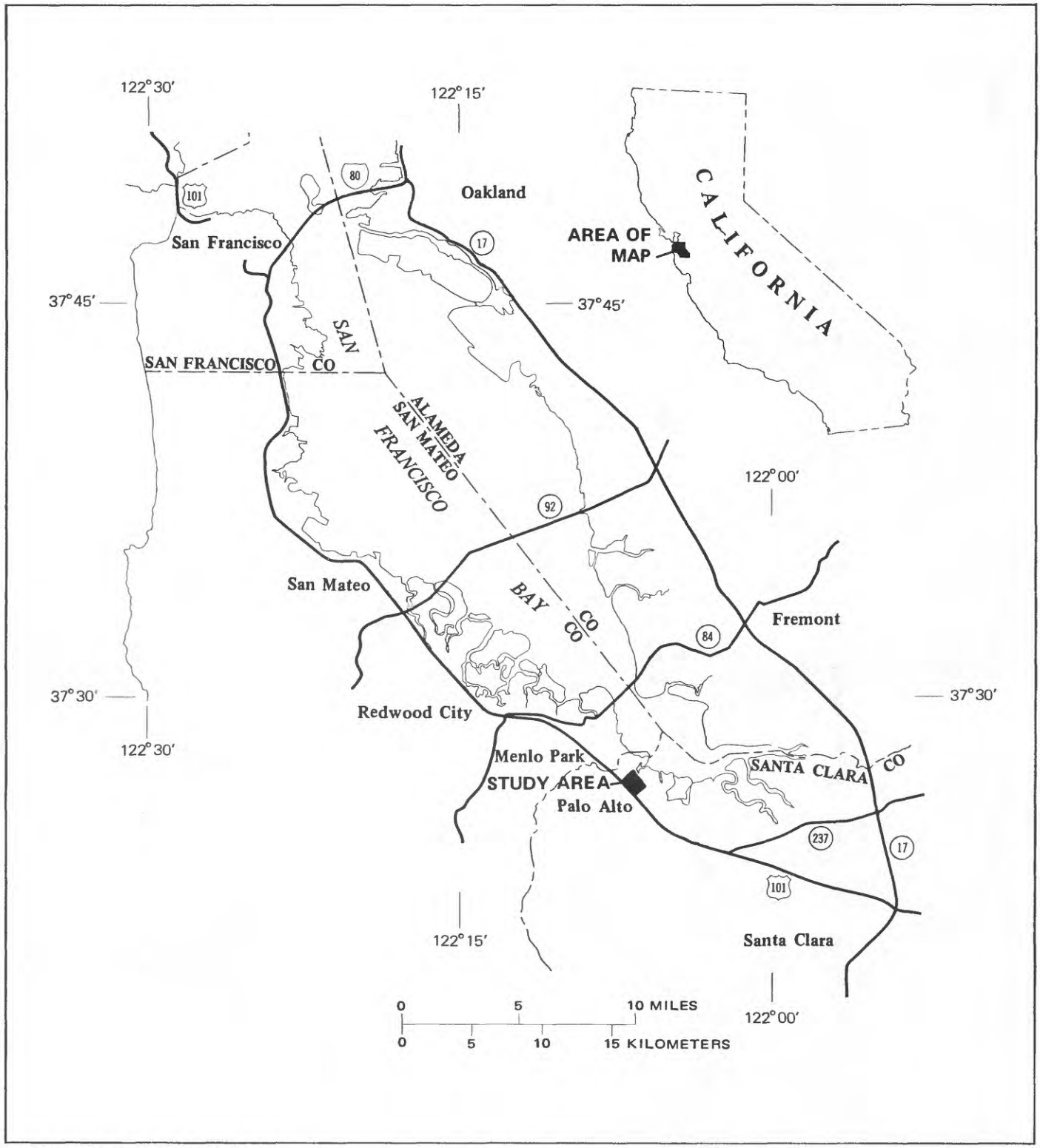

Base from U.S. Geological Survey
San Francisco Bay Region, 1:125,000, 1970

FIGURE 1. – Location of study area.

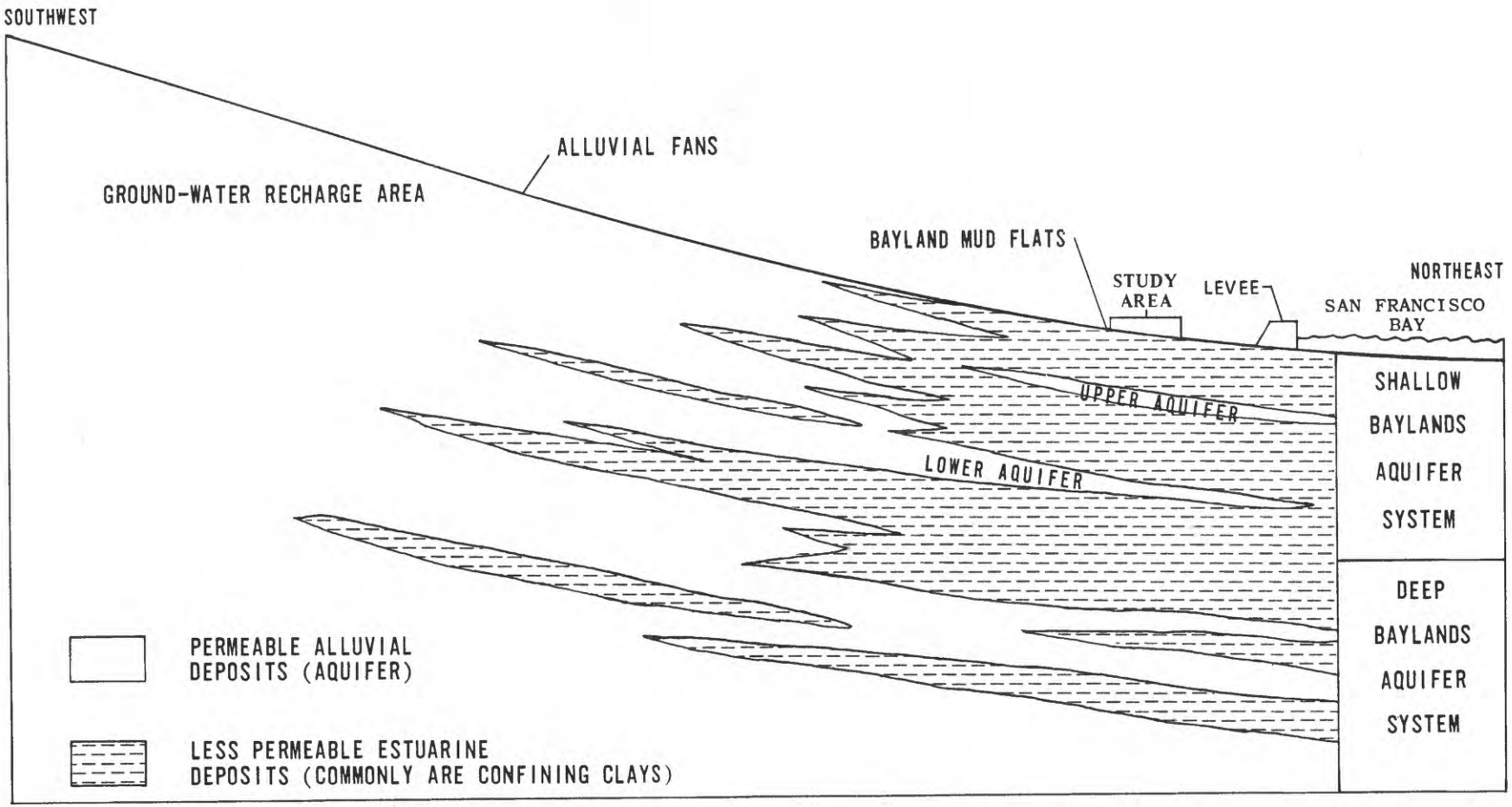

FIGURE 2. – Diagrammatic cross section showing the baylands aquifer systems.

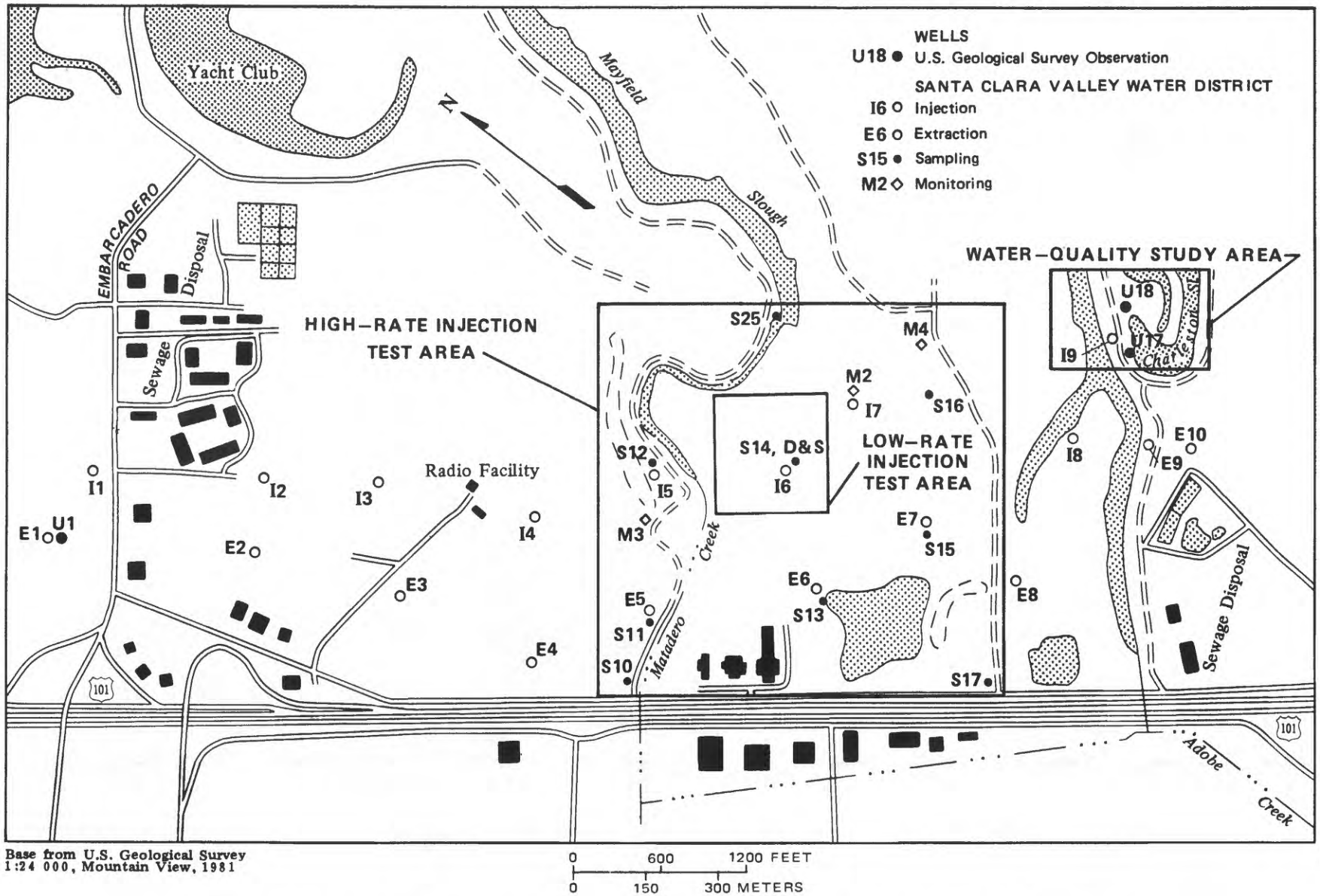

FIGURE 3. – Santa Clara Valley District injection-extraction well network and location of U.S. Geological Survey observation wells. Detail of low-rate injection test area is shown on figure 5.

Previous Work

For a complete description of project objectives, scope, and background information, the reader is referred to the preliminary report (Hamlin, 1983). Initial studies of the area and development of the injection-extraction network were completed by Jenks and Adamson (1973) and Brown and Caldwell (1974). Stanford University evaluated the feasibility of injecting reclaimed water for ground-water recharge; the study concentrated on the behavior of introduced organic constituents in the shallow aquifer system (Roberts and others, 1978). These studies have concentrated on injection well I1 (fig. 3). More recently, a transport model was developed for the shallow baylands aquifer system (Valocchi and others, 1981).

Purpose and Scope

Saline water is the most common pollutant in fresh ground water (Todd, 1980, p. 494). One of the most effective methods of alleviating and controlling this form of pollution is ground-water recharge by injection. The Santa Clara Valley Water District has chosen this method for use in the Palo Alto Baylands shallow aquifer system. Evaluation of this injection-extraction network may help similar operations elsewhere. The purpose of this report is to describe (1) the factors affecting injection efficiency, particularly well and aquifer clogging, and (2) the three-dimensional migration paths of injection and ground water. Evaluation of these factors provides an indication of the degree of success of the ground-water recharge system. The area of this study is contained within the Santa Clara Valley Water District's injection-extraction well field (fig. 3). Observation wells in the vicinity of injection wells I6 and I9 were used to monitor hydraulic and chemical changes in the shallow baylands aquifer system. These data, along with additional information from Stanford University studies at well I1 (Roberts and others, 1978), were used to describe the shallow baylands aquifer system within the well field. General geologic and hydrologic relations within the well field have been described (Hamlin, 1983). Hydraulic and chemical analyses were completed at injection wells I6 and I9 (fig. 3) during winter 1980 through autumn 1981. The combined effects of the geochemistry and hydraulics must be considered in an evaluation of the performance of the injection operation.

Acknowledgments

The author wishes to express his gratitude to those who helped in the preparation of this report. Allen Moench, U.S. Geological Survey, has given invaluable help in the hydraulic analysis. Santa Clara Valley Water District personnel provided extensive assistance with field work. L. Niel Plummer, U.S. Geological Survey, provided an interpretation of the interactions of ground and injection water.

GEOLOGY

History

The aquifer system is complex and heterogeneous within the study area. The upper (20-foot) and lower (45-foot) aquifers are separated by a leaky clay layer formed from estuarine mud. Lithologic variations may be related to the recent geologic history of the San Francisco Bay area. Responding to sea-level fluctuations and tectonic movement, a changing depositional environment resulted in the present stratigraphic relations. The upper and lower aquifers correspond to Holocene and late Pleistocene alluvial deposits, respectively. The baylands aquifer system was developed during the Quaternary period. While the lower aquifer materials were being deposited, the sea level stood several hundred feet below its present elevation. A large river flowed through the bay region as the lower aquifer was deposited in a freshwater fluvial environment about 20,000 years ago. The sea level began to rise about 15,000 years ago, and the "infant" San Francisco Bay entered the Golden Gate about 10,000-11,000 years before present time. At the same time, the upper aquifer was deposited in a predominantly freshwater environment. The growing bay reached the vicinity of Menlo Park about 8,000 years ago, and subsequent shoreline changes have been more gradual because of a decrease in the rate of sea-level rise. Progradation of mudflats and salt marshes began when the rate of sediment accumulation exceeded the rate of sea-level rise.

Lithology of the Shallow Baylands Aquifer System

The shallow baylands aquifer system is composed of interlayered alluvial and estuarine deposits. Most of these materials were deposited during Holocene time (within the last 10,000 years). A thick confining bed consisting predominantly of water-saturated clay and silty clay forms the base of the aquifer system. Overlying these estuarine deposits is the lower (45-foot) aquifer typified by coarse-grained alluvial deposits. Streams in the marsh environment formed natural levees composed of silts and clays (Helley and La Joie, 1979). The stream-levee morphology is evident in the lower aquifer structure near well I6 in a former stream channel (Hamlin, 1983). A leaky clay layer above the lower aquifer generally interfingers and grades into the alluvial deposits. Recent estuarine clay deposits containing framboidal pyrite (bio-organic deposition) are characterized by a "rotten-egg" odor from hydrogen sulfide. The upper (20-foot) aquifer overlying the leaky clay layer is generally finer grained than the lower aquifer. A narrow band of fine-grained, salt-affected alluvium is exposed along the margin of the Palo Alto marsh (Helley and La Joie, 1979).

HYDROLOGY

Occurrence of ground water

The aquifer system is shown in a four-layer conceptual diagram in figure 4. The upper aquifer (layer 1) contains saline water in a water-table environment that has good hydraulic connection, promoted by an extensive root system, to the land surface. This aquifer rests on a leaky-clay unit (layer 2) locally providing limited hydraulic connection with the lower aquifer (layer 3), which contains denser, highly saline water. Heads are generally higher in the confined lower aquifer than in the unconfined upper aquifer. The lower aquifer rests on an impermeable thick clay zone (layer 4) that isolates it from a deeper freshwater aquifer. The intermediate clay layer is not continuous throughout the study area. Local variations in the depositional and erosional environment have produced "windows" of alluvial material in the clay layer, which provide good connection between the upper and lower aquifers.

Aquifer System Hydraulic Characteristics

Hydraulic properties of the aquifer system (fig. 4) have been estimated previously (Hamlin, 1983). The uppermost aquifer is treated as a constant head source to simplify the analytical mathematical assumptions, and this assumption is sufficient for the time frame of the aquifer tests. A deep root zone provides good hydraulic connection to the land surface. An intermediate-depth leaky-clay confining bed separates the upper aquifer from the lower. This lower aquifer, the focus of study, is underlain by an impermeable clay layer. To reduce the numerical complications of three-dimensional analysis, ground-water flow is assumed to be horizontal in the upper and lower aquifers and vertical in the intermediate leaky-clay layer.

The modified Hantush method (Hantush, 1960) was used in the analysis of drawdown data to estimate transmissivity, vertical permeability, and storage coefficient. Inherent error is associated with the discrepancy between actual conditions and mathematical assumptions. The assumptions (Theis, 1935) include the following: (1) The aquifer is homogeneous and isotropic, (2) the aquifer has an area of infinite extent, (3) the pumped well has an infinitesimal diameter, (4) the well penetrates the entire thickness of the aquifer, and (5) the water removed from storage is discharged instantaneously with decline in head. Previously determined values for aquifer parameters in the lower aquifer were 960 ft^2/d for transmissivity and 5×10^{-4} for storage coefficient (Hamlin, 1983). The vertical hydraulic conductivity in the intermediate clay confining bed was estimated to be 0.08 ft/d.

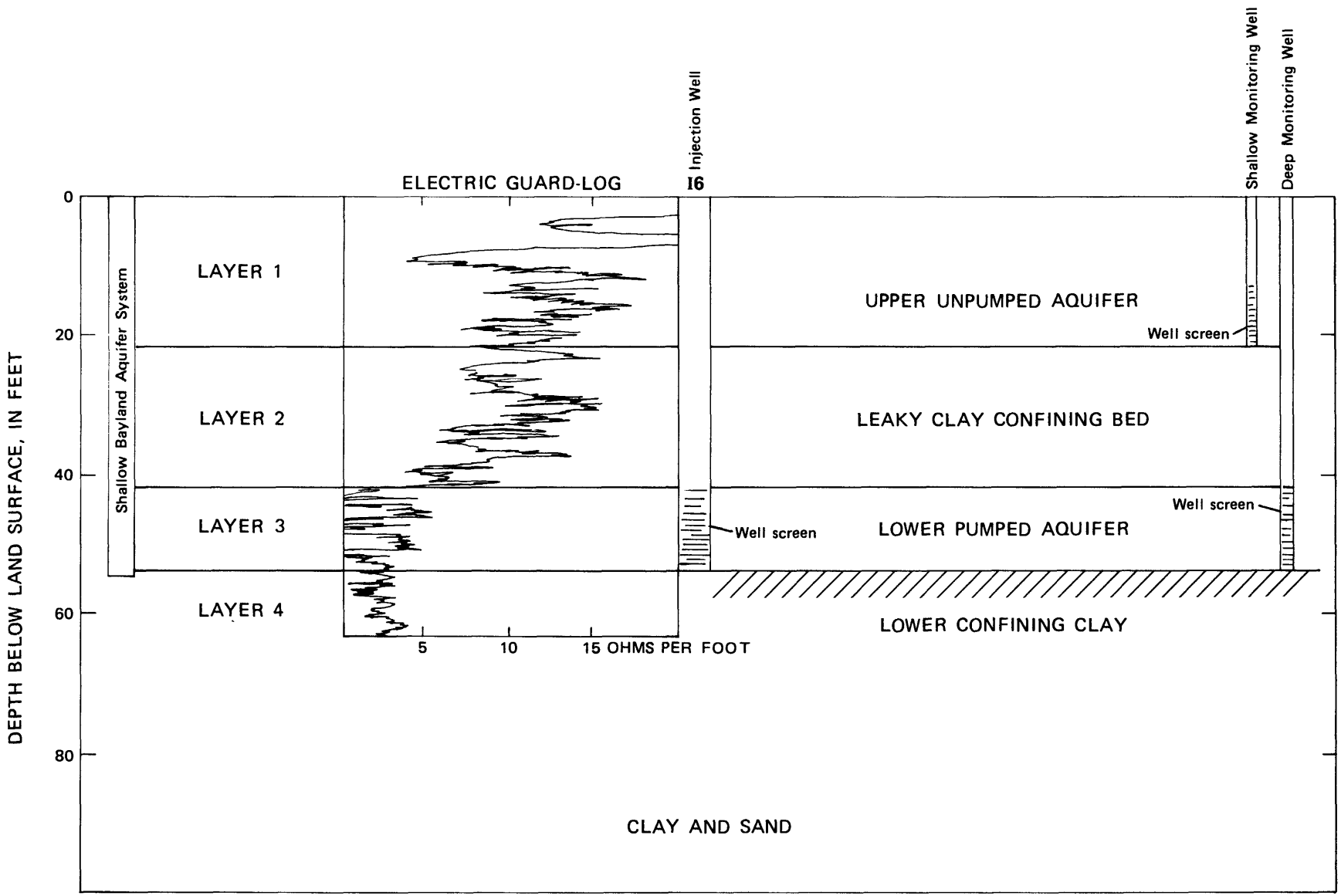

FIGURE 4. – Four-layer conceptual diagram of the shallow baylands aquifer system and log showing variation in electrical resistance with depth.

Hydraulic Analysis of Injection at Well I6

Method of Study

The hydraulic effect of 10 gal/min injection in the lower aquifer at well I6 was monitored in 15 observation wells installed by the Geological Survey. These observation wells, which were constructed with PVC pipe 1 inch in diameter, were perforated in the lower aquifer and placed within a 400-foot radius of injection well I6 (fig. 5). The network was designed to determine areal flow direction from variations in water level within the lower aquifer during injection. Water-level and electrical-conductivity data were used to monitor possible changes in aquifer hydraulic and chemical properties and injected-water flow directions. An initial 10 gal/min extraction test was run in September 1980 to provide a baseline indicator for clogging. Head data collected during later injection tests (with an injection rate of 10 gal/min) were compared to the background test data to detect changes in aquifer and well properties. Several 10 gal/min injection tests were run at well I6 over a 6-month period. Specific-capacity plots were constructed and compared for each of these tests, which lasted from 1 to 3 months. This period of testing, which was done to detect changes in the well or aquifer hydraulic properties, was completed in June 1981.

The second period of injection in the lower aquifer at well I6 involved a larger area of study (a radius of about 2,000 feet) and higher injection rate (100 gal/min). The objectives of this segment of study were (1) to assess the impact of high-rate injection on the aquifer water quality and (2) to determine the hydraulic changes in the well and (or) aquifer as a result of the increased injection rate. Well sites used to monitor high-rate injection were M2, M3, M4, S10, S11, S12, S13, S15, S16, S17, and S25 (fig. 3). Water level, pH, temperature, and chloride concentration were determined at these sites. At most of the monitoring locations, two wells were installed side by side and perforated in the upper (20-foot) or lower (45-foot) aquifers, which allows study of the hydraulic relation between the upper and lower aquifer units and changes in water quality.

An injection rate of 100 gal/min was maintained for about 2½ months. About 10 million gallons of reclaimed water were injected during the test. Water level, temperature, pH, and chloride-ion measurements were made at 25 observation wells during injection. Samples for chloride-ion measurements were collected by airlift from the Water District's 3-inch-diameter observation wells. Electrical conductivity was monitored until a constant value was obtained during pumping, at which time the sample was taken. Samples were analyzed at the Survey's Central Laboratory in Arvada, Colo. Pumping tests were run before and after this period of injection to determine changes in well performance.

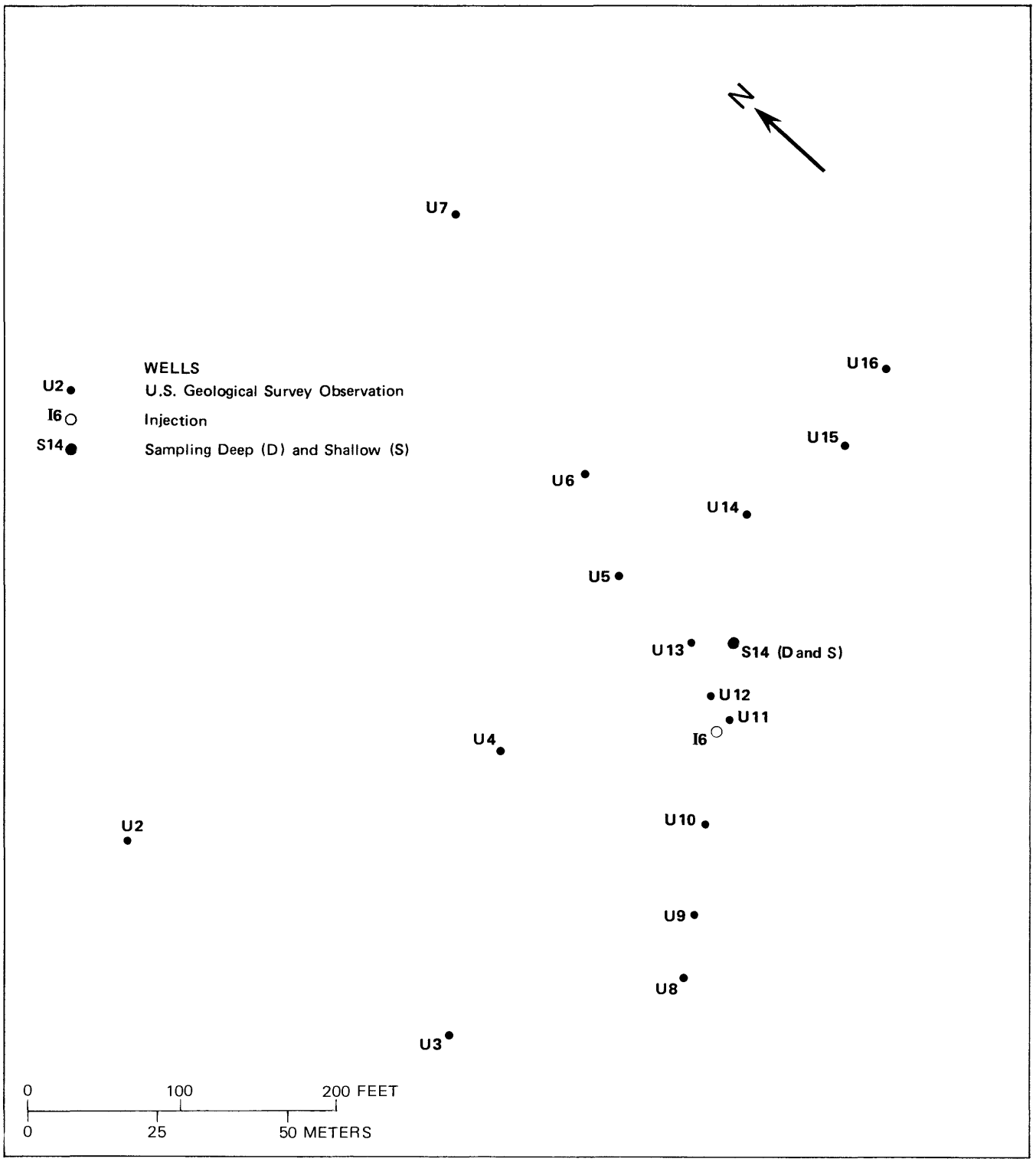

FIGURE 5. – Low-rate injection test area and location of U.S. Geological Survey observation-well network (U-wells) at the Santa Clara Valley Water District injection well I6 and sampling well S14-Deep and S14-Shallow. Location of this test area is shown in figure 3.

Breakthrough on Plots of Hydraulic Conductivity Versus Time

Specific capacity (injection rate/head buildup) versus time for well I6 is shown in figure 6. The most obvious feature of the data from the initial injection test is a rapid decrease in specific capacity between 4 and 10 minutes after the start of injection. This decrease results from the displacement of saline water by injected freshwater. Once saline ground water was locally replaced by freshwater, successive injection tests (freshwater into freshwater) followed and extended the upper (early-time) section of the curve, which shows no downward break in the slope of the specific-capacity curve. Since pressure and other injection parameters apparently remained constant during the succeeding tests, the change in water level might result from the density difference of approximately 3.5 percent between injection water (1.000 g/cm^3) and saline ground water (about 1.035 g/cm^3).

If the height of the water column, z, is measured from the bottom of the lower aquifer, the change in z may be explained in terms of the fluid potential, ϕ, which remains constant at equivalent injection time between tests. Fluid potential, ϕ, is derived from the sum of three terms: gravitational potential energy, kinetic energy, and elastic energy of the fluid. Flow velocities for porous media are extremely low, so that the kinetic-energy term may be neglected (Freeze and Cherry, 1979); since the fluid pressure has remained constant at specific injection time between injection tests, the elastic-energy term may also be omitted. Fluid potential therefore is roughly equivalent to potential energy, mgz, which may also be written as ρgz for a unit volume, where g = gravitational acceleration, m = mass of the fluid, and ρ = fluid density. The freshwater elevation, z_f, may then be calculated on the basis of the difference in density between freshwater (ρ_f) and saline ground water (ρ_s), using the initial saline water elevation, z_s, at a specified point in time:

$$\rho_s \; g \; z_s = \Phi = \rho_f \; g \; z_f.$$

Gravitational acceleration, g, may be factored from the relation, leaving

$$\rho_s \; z_s = \rho_f \; z_f.$$

Inserting measured water densities and saltwater elevation from the injection test data, the result is (1.035 g/cm^3)(45 feet) = (1.000 g/cm^3) z_f.

Rearrangment produces

$$z_f = (1.035)(45 \text{ feet}) = 46.58 \text{ feet},$$

an increase in water-column height of about 1.6 feet when saline water is replaced by freshwater. The change in water elevation interpreted from figure 6 is about 1.5 feet, which was determined by extending the early-time curve and comparing it with the curve produced after freshwater replacement of saline water. The close agreement between these values indicates that fluid-density difference is the primary factor in the observed effect on the specific-capacity curve. The duration of this phenomenon in the injection well, from 4 to 10 minutes or 40 to 100 gallons injected, represents total replacement of saline ground water in the well casing by less-dense, injected freshwater. Larger changes in water level would be observed in systems with greater water-column depths and (or) fluid-density difference.

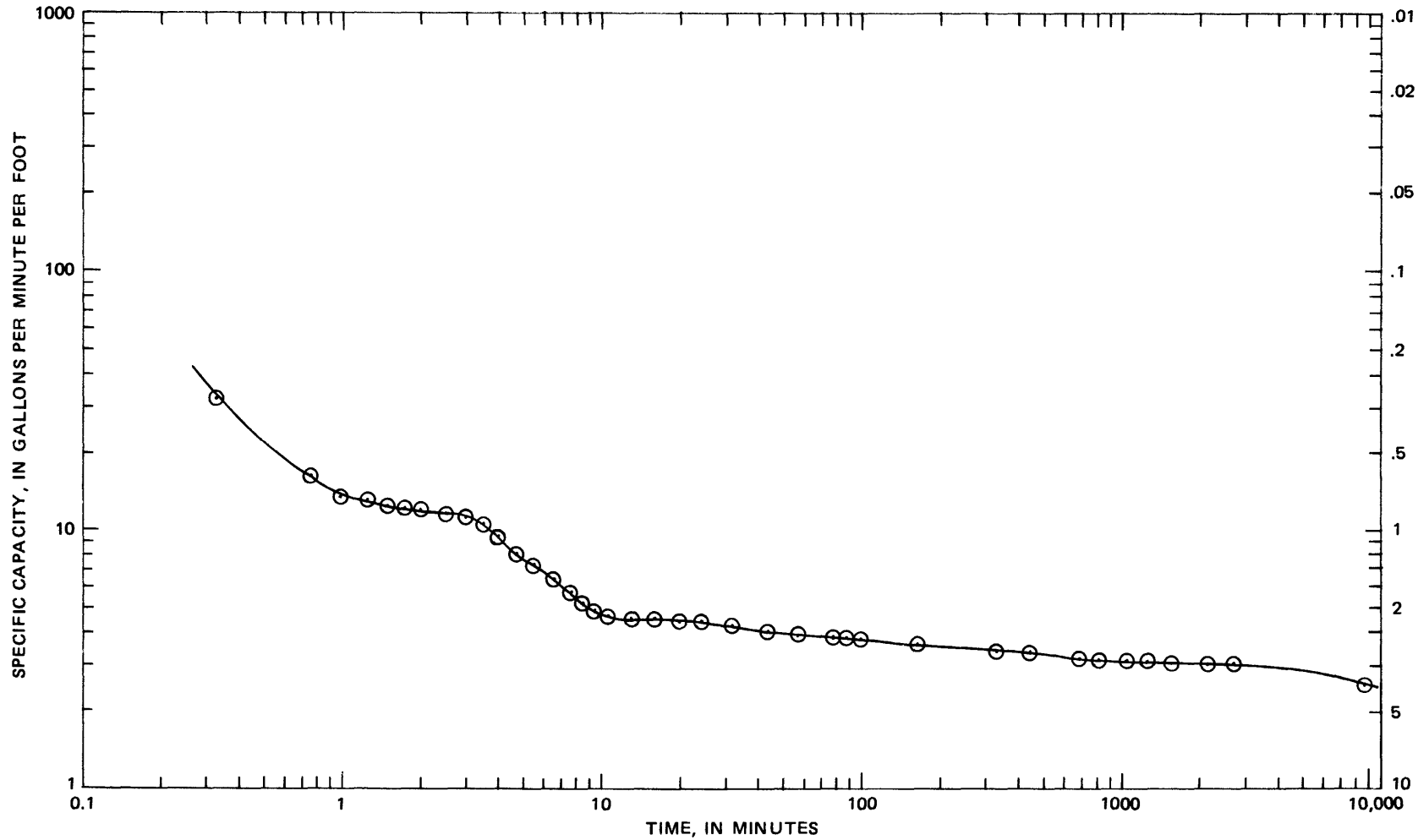

FIGURE 6. — Initial low-rate (10 gallons per minute) injection-test data at well I6.

Similar behavior to that of well I6 was noted at several observation wells, for which specific-conductance values are plotted concurrently with water-level data on figures 7 and 8. The displacement of saline water is confirmed by the specific-conductance breakthrough curve, which corresponds to the arrival of freshwater at these wells. Where the density of injected and native water contrasts significantly, the arrival of the injection water may be monitored entirely through water-level data.

Water-Level Variations During Low-Rate Injection

The contours of the ground-water surface in the lower aquifer are defined primarily by the aquifer properties and the distribution of ground-water discharge and recharge areas. These factors strongly influenced injection-water flow, and subsequent water-density variation influenced the observed water levels. Figure 9 shows the water-level contours in the vicinity of well I6 just prior to injection. At this time (December 1980), after an extended dry period, the hydraulic gradient was in a southwesterly direction, inland from the bay. During the previous October, the gradient was to the southeast, indicating recharge from Matadero Creek to the north (Hamlin, 1983). The change in direction of the hydraulic gradient is due in part to modification of the tidal-gate operating schedule that controls inflow to the sloughs from the bay. During the later period of testing, the tidal gates allowed influx over a wider range of tidal levels, which raised slough and ground-water levels in response to increased hydraulic pressure and recharge.

Water-level contours about 2 days after injection began are shown in figure 10. The area of close contours (steep slope) between wells U11 and U12 corresponds to the location of the interface of injection and saline water (figs. 7 and 8). The event is shown near completion at well U11 and is just beginning at well U12. The arrival of the injection water is characterized by a rapid rise in water level, which can be visualized as an expanding ellipsoidal "scarp" surrounding the injection well.

The first 10 gal/min injection test ran for 47 days until storm floodwaters caused a short circuit in the electrical system controlling the injection field, which resulted in shutdown. Injection resumed about a month later, and the water-level contour map for February 24, 1981, shows a double mound (fig. 11). The adjacent dome in the ground-water surface to the east, a remnant of the previous period of injection, resulted from the density contrast between injected water and native ground water. The dome, a freshwater bubble, preferentially travelled down a buried stream channel in the lower aquifer to the southeast (Hamlin, 1983). At this time, winter recharge evidently reversed the inland ground-water gradient (dry season) shown in figure 10, resulting in the observed migration direction. In the following section of this report, this paleochannel morphology is described in terms of aquifer particle-size distribution. Resumption of injection heightened this effect by increasing the hydraulic gradient toward the bay, pushing the former injection mound in this direction. This phenomenon indicates little and (or) very slow mixing of the injected water and briny ground water. Evidently, a well-defined interface exists between the two, particularly during the initial phases of injection.

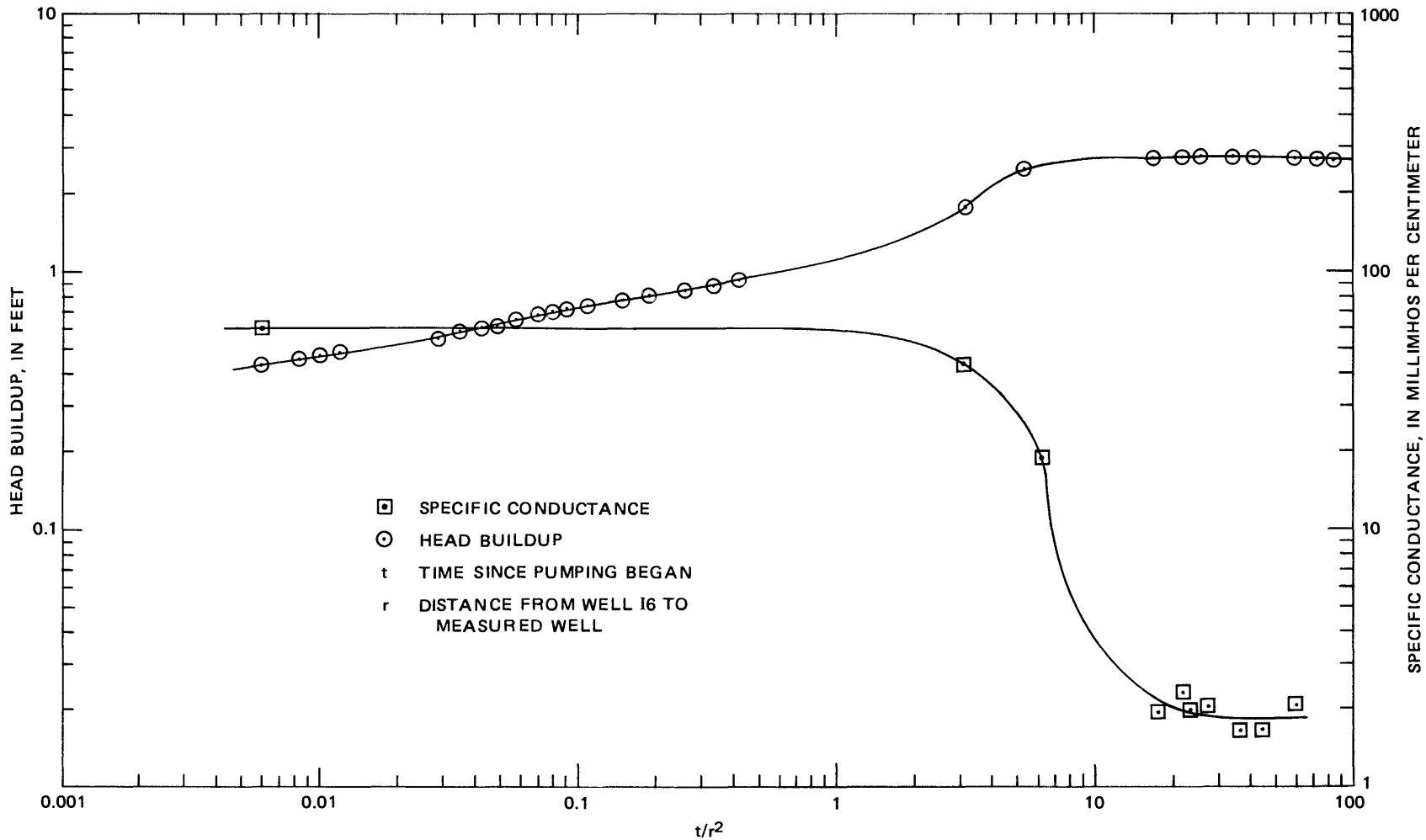

FIGURE 7. – Specific-conductance and water-level data at well U11.

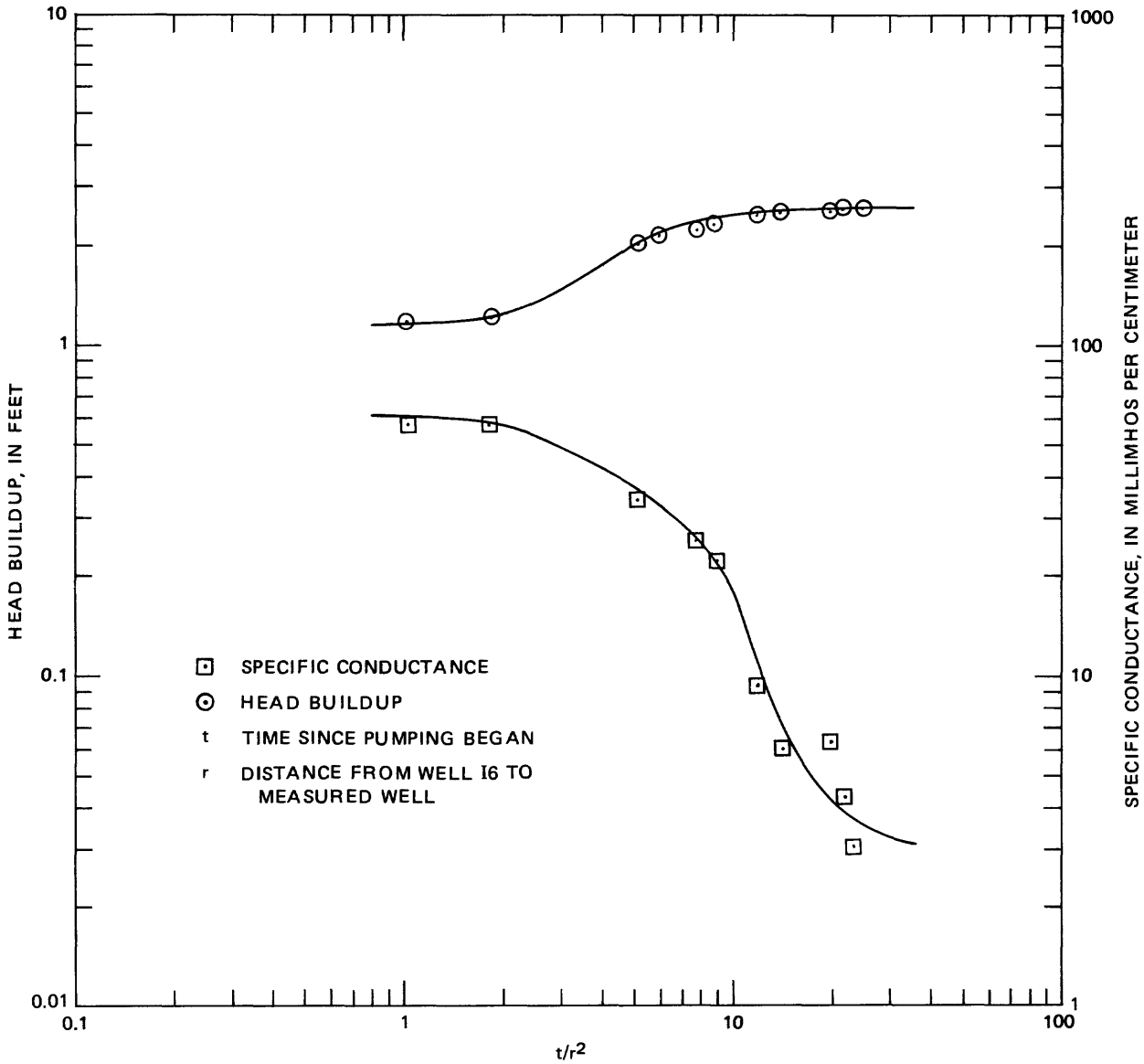

FIGURE 8. – Specific-conductance and water-level data at well U 12.

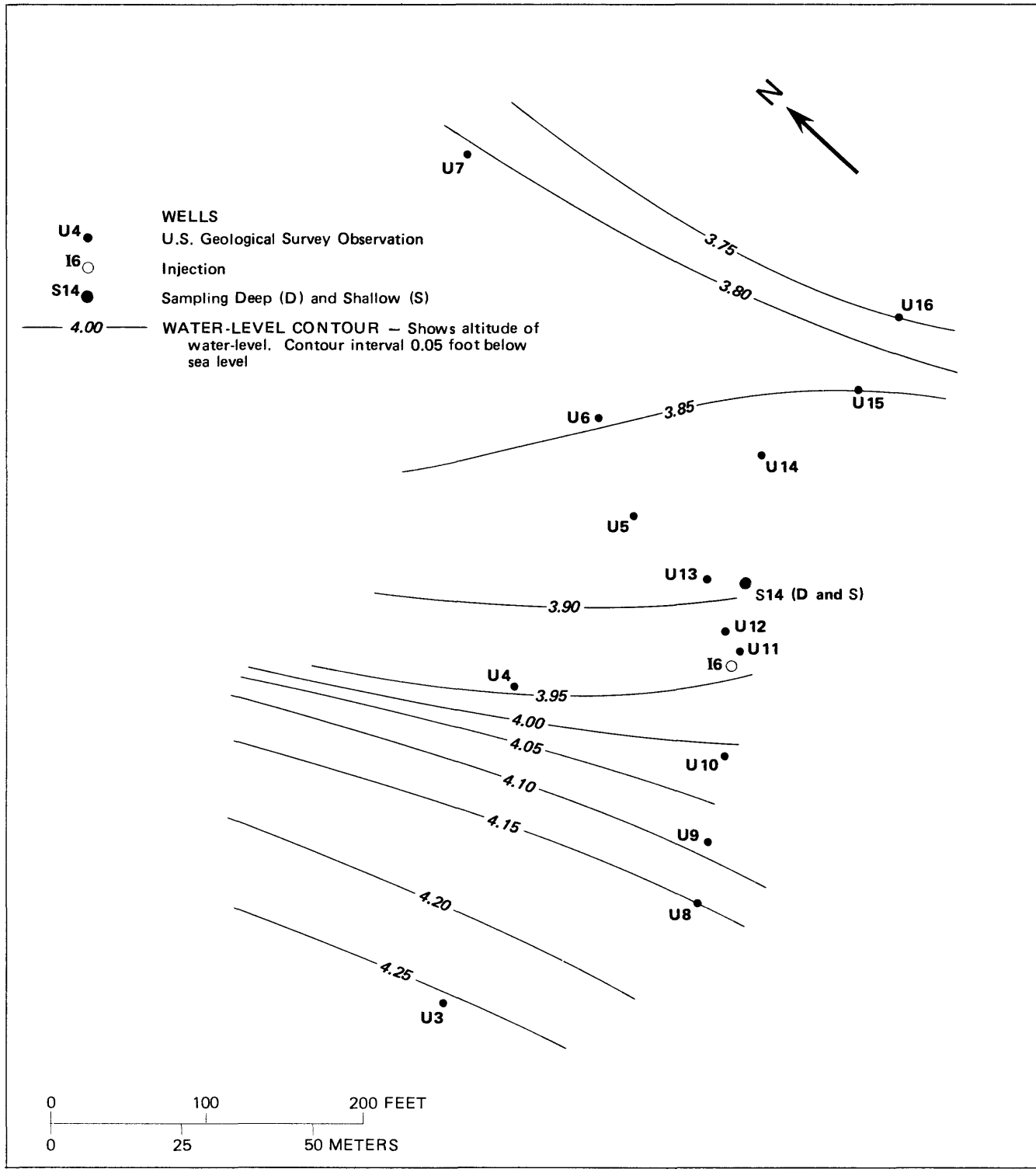

FIGURE 9. – Water-level contours for the lower (45-foot) aquifer prior to injection at well I6 in the low-rate injection test area. Location of this test area is shown in figure 3.

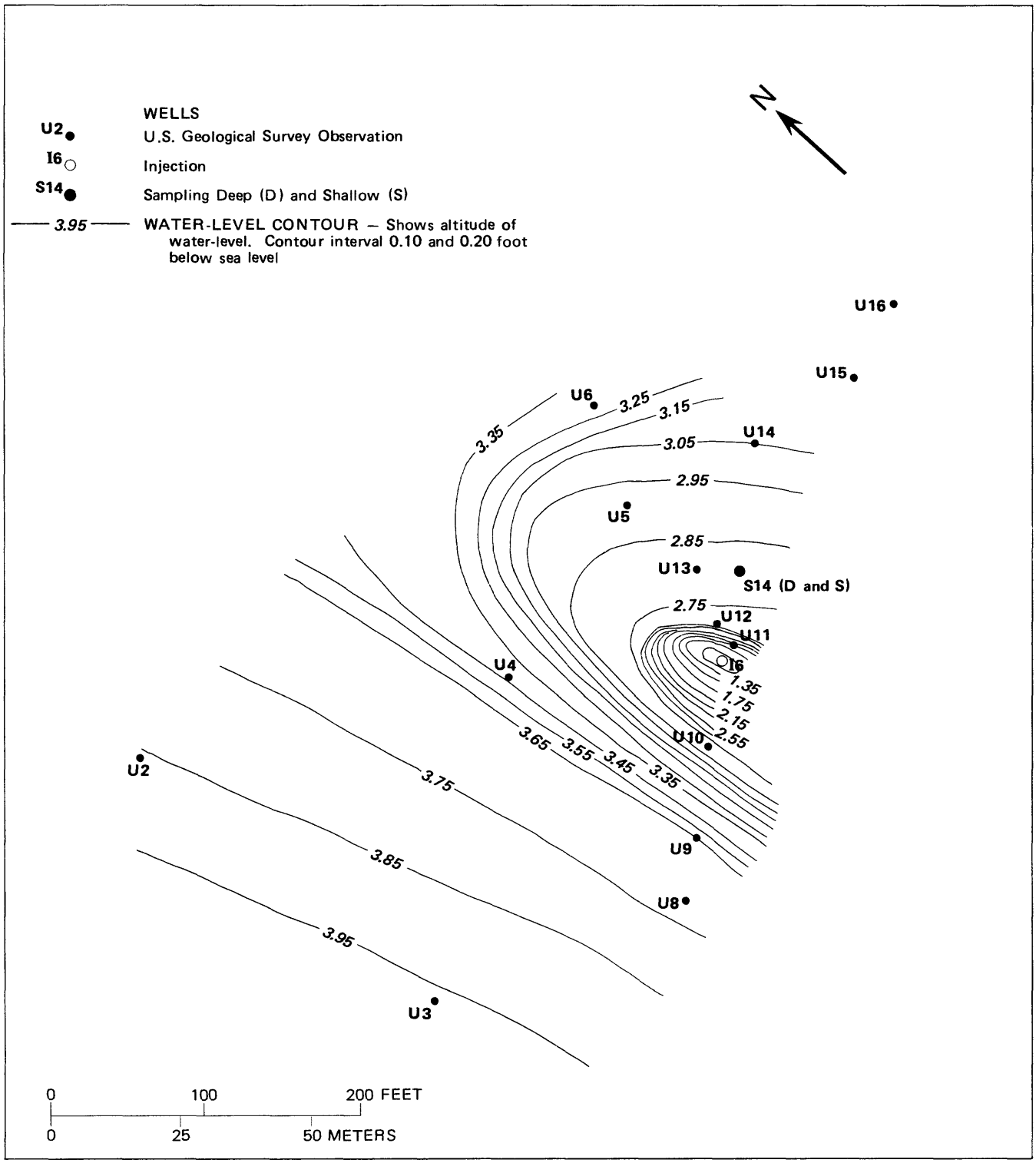

FIGURE 10. – Water-level contours for the lower (45-foot) aquifer 3,015 minutes after start of injection at well I6 in the low-rate injection test area. Location of this test area is shown in figure 3.

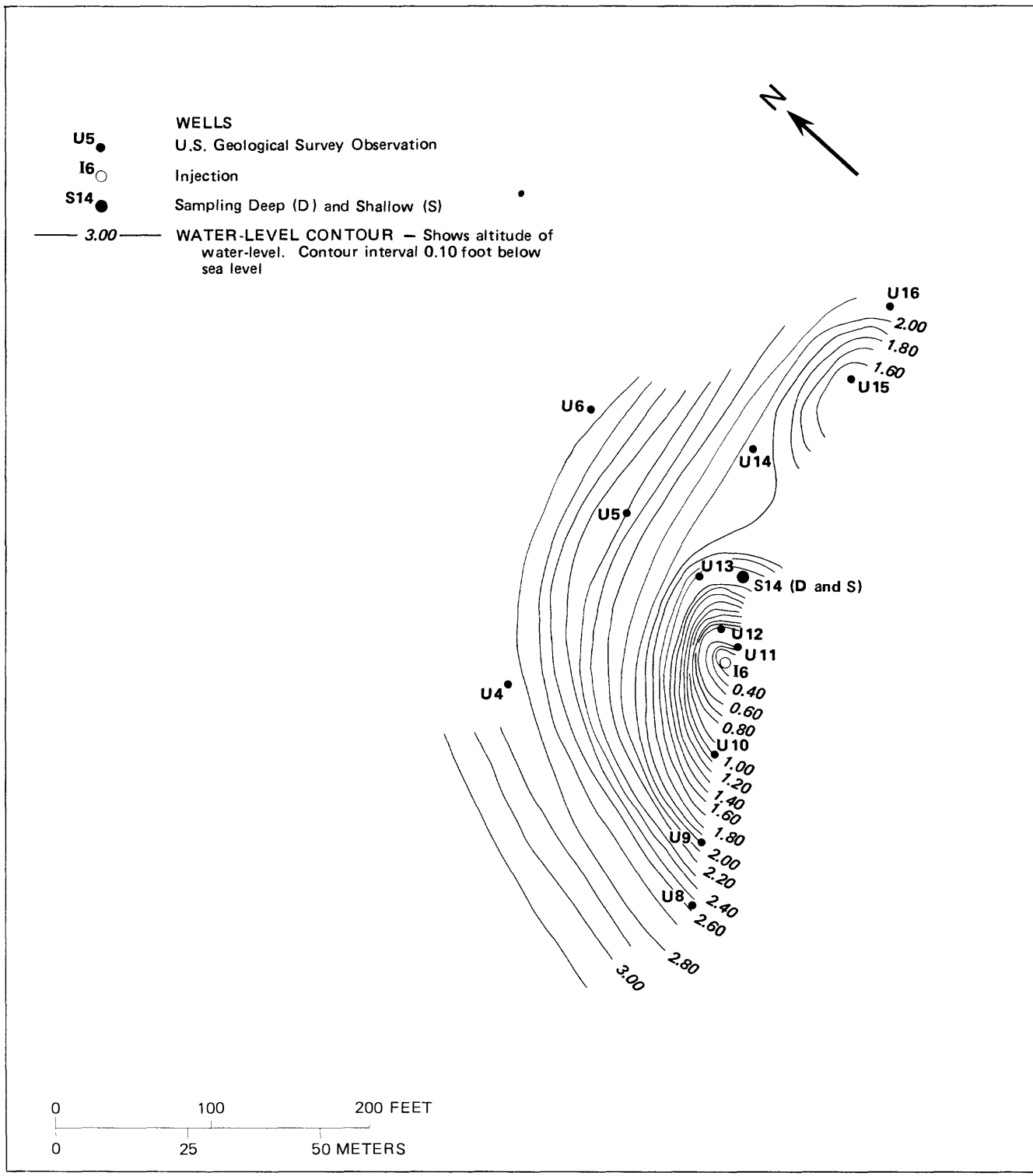

FIGURE 11. — Water-level contours near well I6 after the start of the second period of injection, February 24, 1981, in the low-rate injection test area. Location of this test area is shown in figure 3.

Particle-size Distribution, Aquifer Permeability, and Ground-Water Flow

A buried channel containing coarse-grained deposits was located on the basis of particle-size data (Hamlin, 1983). This feature runs roughly northwest-southeast, and it was delineated (fig. 12) by mapping the location of coarse material (containing >90 percent sand and gravel) in the lower (45-foot) aquifer. The coarsest material was found along the axis of this structural trough, bounded on either side by finer, less permeable material. Injection well I6 is located on the axis of this feature. The injection water preferentially migrated along this path. Control over injection-water migration is primarily related to variations in permeability, which varies with particle size and distribution and the continuity of pores. Permeability in the lower aquifer may be inferred from figure 12, which was developed from particle-size data from core samples taken during the installation of the observation-well network.

Injection water may change the initial permeability of the aquifer system. Chemical reactions between the two unlike types of water may cause precipitation or dissolution within the aquifer. Dilution of saline water by injection water can shift chemical equilibria, resulting in dissolution of chemical precipitates and possibly improvement of permeability. On the other hand, permeability may be reduced by clay swelling resulting from cation exchange and by filter-packing of suspended materials.

Water-Level and Chloride Variation During High-Rate Injection

Water-level variation near well I6 resulted from injection head buildup and fluid-density change reflecting replacement of ground water by injected water. For the most part, water-level increases distant from well I6 were related to increased pressure rather than fluid-density change resulting from the arrival of injected water, which was not observed in the distant wells. Similarly, chloride content in most shallow wells increased gradually, most likely because of brine migration induced by the injection-produced hydraulic gradient. Data plots of water-level change and chloride are presented in Appendix A.

The line of extraction wells inland from the bay and parallel to the line of injection wells (fig. 3) was designed to form a hydraulic trough to prevent injection-induced inland migration of saline ground water. Coordination of pumping at these wells forms an extraction barrier (linear hydraulic sink). Two factors reduce the efficiency of the extraction barrier for removing and containing the brine: (1) Heterogeneity of the aquifer system, which results in channeling of flow; and (2) gaps in the extraction networks from inoperative or improperly installed wells. By operating the extraction wells asynchronously with the injection wells, a trough can be formed without risk of contamination of adjacent freshwater. The injection wells can then be operated intermittently to dilute and flush out saline ground water.

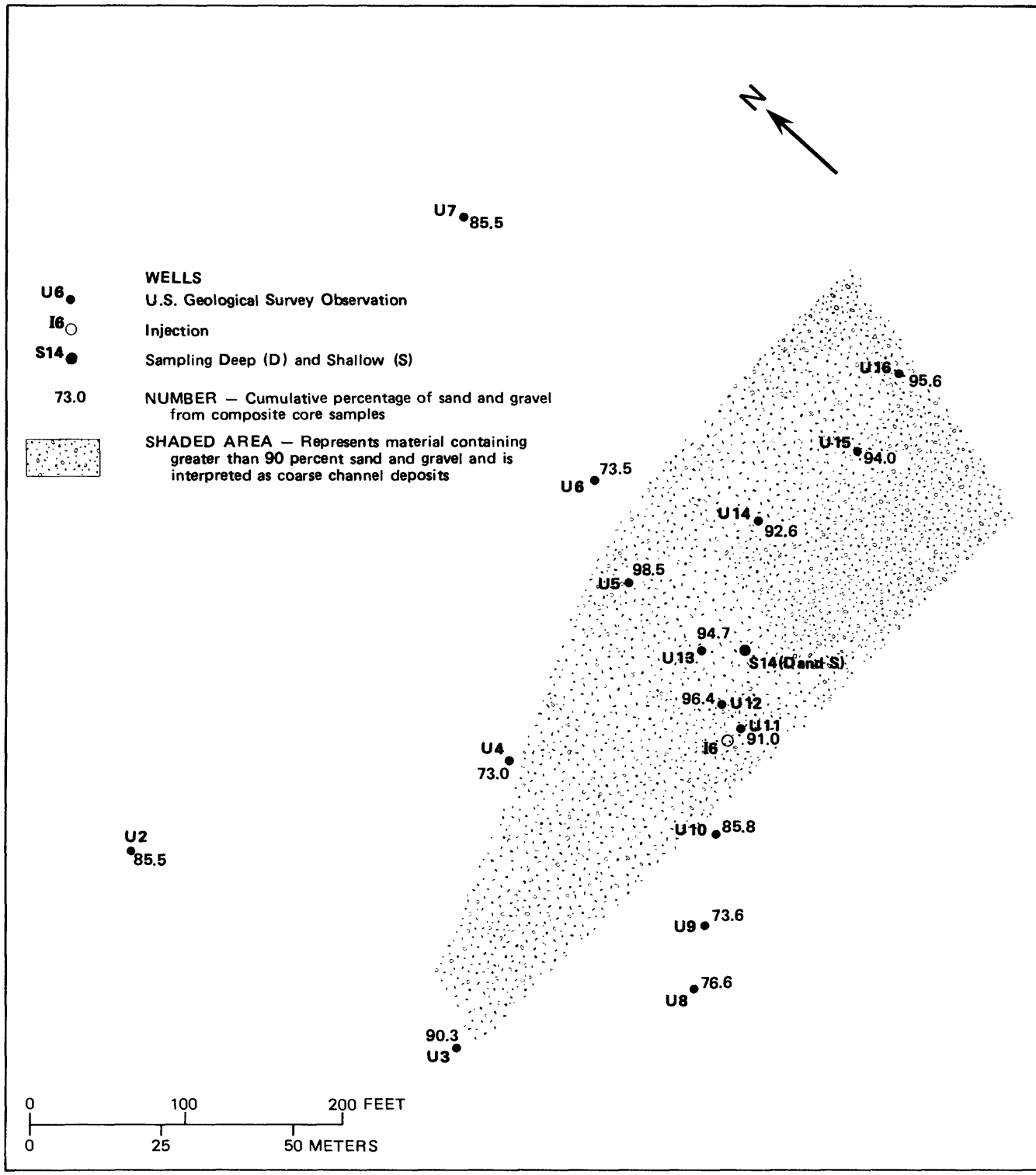

FIGURE 12. — Particle-size distribution in the lower (45-foot) aquifer in the low-rate injection test area. Location of this test area is shown in figure 3.

Most dual-well sites in the area south of Matadero Creek showed apparently unrelated chloride concentrations and water levels between wells at the same site. North of Matadero Creek, however, wells M2, S10, S11, and S12 behaved identically with respect to water level and chloride variations. Evidently, these dual wells, screened in the upper and lower aquifers, are hydraulically connected. Two explanations are possible: (1) The discontinuity of the confining clay in the area allows hydraulic connection between the upper and lower aquifers, and (2) the wells may have been perforated inadvertantly in the same aquifer. The second possibility is the most likely, as illustrated in figure 13, which shows identical values for chloride and water-level data in upper and lower wells. Most of the study area lies to the south of Matadero Creek, where the leaky clay layer provides limited hydraulic continuity between the upper and lower aquifers. Injection causes head buildup in the lower aquifer, which promotes increased leakage through the clay layer. As the reclaimed water enters the lower aquifer, a pressure mound forms around the injection well. The hydraulic gradient between lower and upper aquifers may reverse, resulting in upward flow through the confining clay layer. Initially, salinity increases with depth, but injection of freshwater into the lower aquifer locally reverses this trend. As injection proceeds, saline water may be locally forced out of the confining clay layer and into the upper aquifer. Continuation of this process can increase salinity in the upper aquifer, presumably until freshwater flushes the clay layer. Clay swelling, which reduces vertical permeability, may slow this process. Evidence of increasing salinity in the upper aquifer is seen in a plot of chloride concentration versus time at a well about 50 feet from the injection well (fig. 14). This trend may be expected to continue until freshwater penetrates the clay layer, after which the chloride concentration presumably decreases toward the freshwater concentration.

Specific-Capacity Variation and Clogging

Specific-capacity plots from injection tests before and after high-rate injection of 100 gal/min at well I6 are shown in figure 15. The well actually showed a small improvement in specific capacity. In general, the final specific capacity was slightly higher in the second test, probably as a result of improved permeability in the aquifer and (or) increased well efficiency. Factors possibly responsible for this improvement include (1) flushing of the matrix and (2) chemical dissolution of matrix minerals, specifically calcite, in response to dilution of native water. Data do not indicate clogging of the well or aquifer.

No evidence of clogging of the well or aquifer was found during tests using an injection rate of 10 gal/min. Specific-capacity data for a background extraction test and for an injection test after 2 months of injection are plotted in figure 16. Because specific capacity showed no change between these tests, the well and aquifer system performance, as a whole, also remained constant. It may then be inferred that there was no clogging during injection.

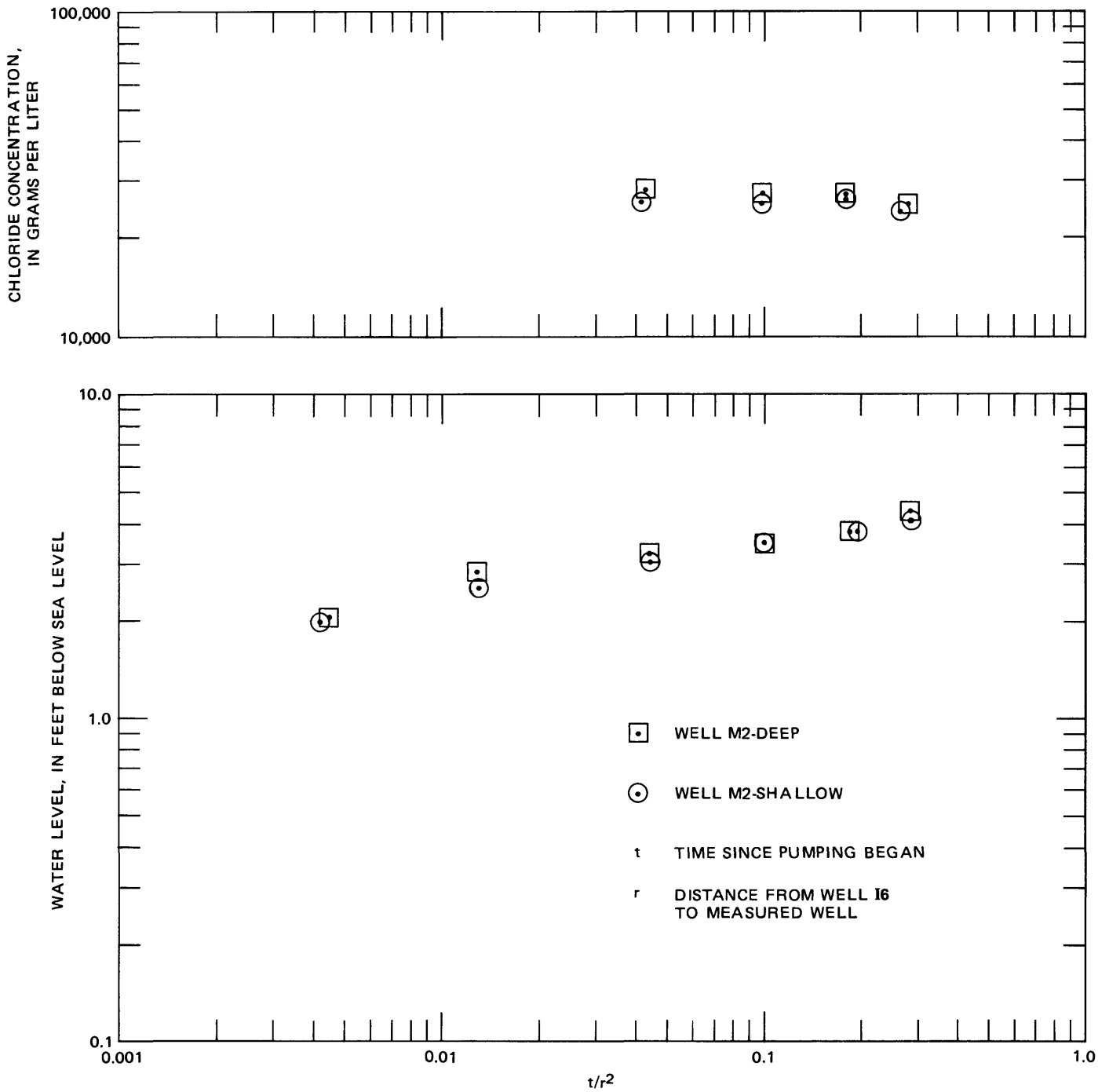

FIGURE 13. – Water-level and chloride data for wells M2-Deep and M2-Shallow.

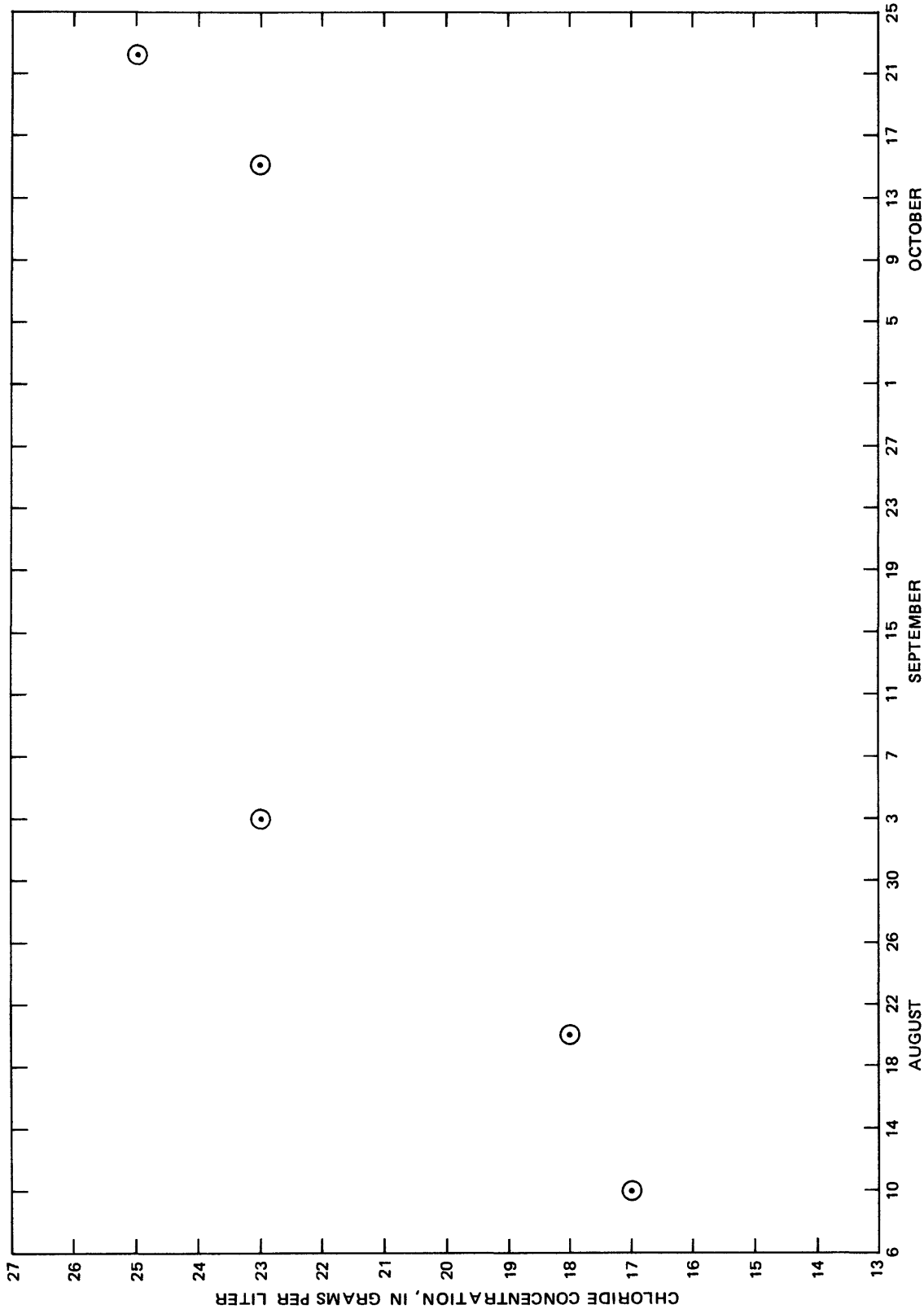

FIGURE 14. – Chloride concentration in the upper aquifer at well S14-Shallow.

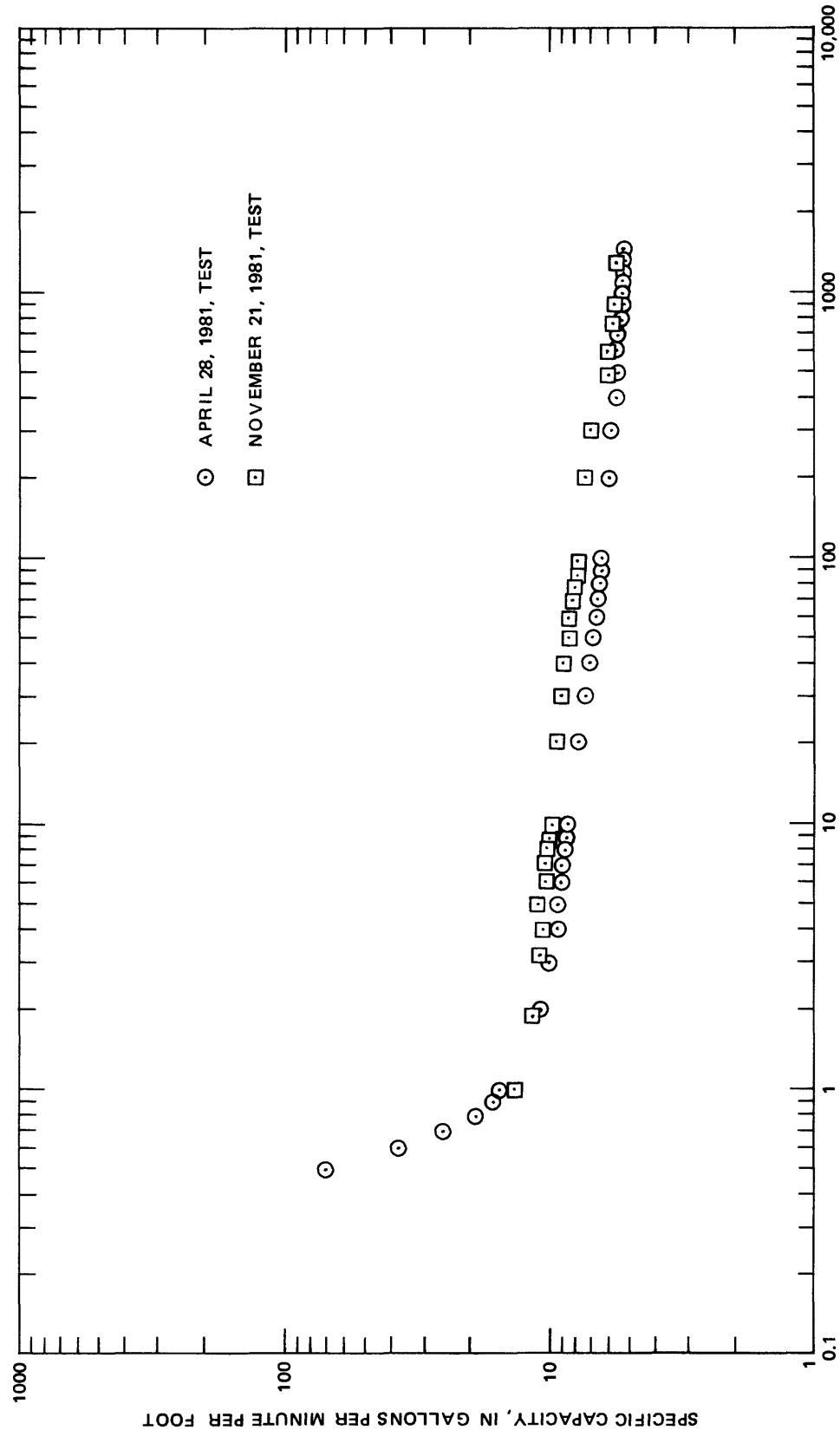

FIGURE 15. — Specific-capacity tests at well I6 before and after 100 gallons per minute injection.

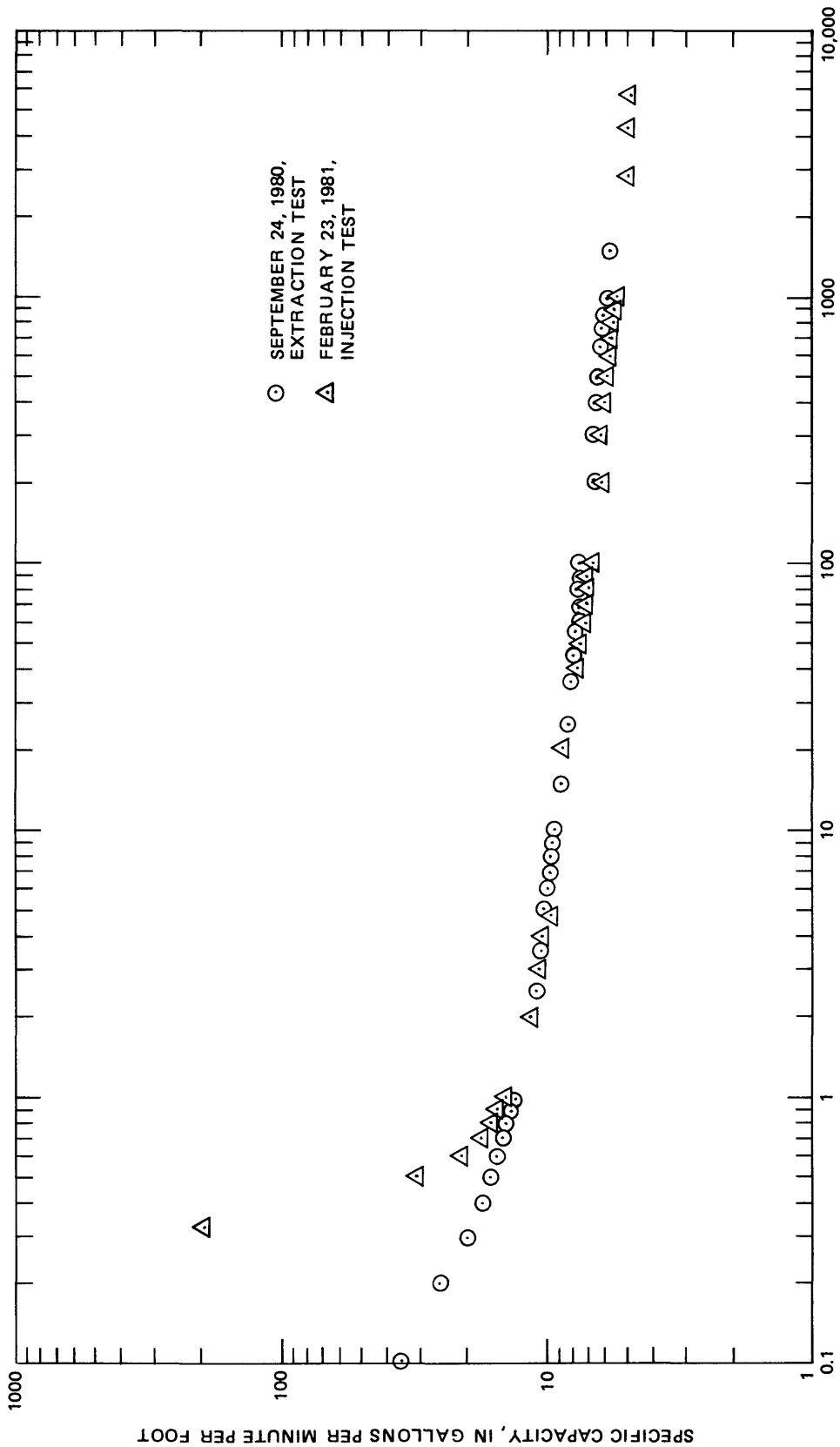

FIGURE 16. – Comparison of specific-capacity data at well I6 from two pumping tests, September 24, 1980, and February 23, 1981.

Genesis of Ground-Water Brine

Highly saline water is present in the shallow baylands aquifer system underlying the Palo Alto marsh. The salinity is greater in the lower aquifer than in the upper aquifer. This salinity difference is indicated in the electric guard log of figure 4 (electrical resistance versus depth). According to chemical analysis, salinity of ground water is up to twice the salinity of seawater, which indicates that concentration must have occurred. The zone of briny ground water underlies the present-day marsh, bounded by the 1850 shoreline (largest extent of bay) to the south and the present shoreline to the north (fig. 17). Alluvial deposits containing efflorescent salts are exposed along the margins of the marsh (the 1850 shoreline), which indicates a former evaporative environment. Marsh development in the last 130 years appears related to the genesis of the ground-water brines in terms of similar distribution and formational environment. An embayment between alluvial fans may have allowed baywater to concentrate as a result of evaporation (Iwamura, 1980).

The stable isotopes $^{18}0$, $^{16}0$, ^{2}H, and ^{1}H, which compose the water molecule, are of special interest in hydrologic studies. The isotope ratios are expressed, in delta units (δ), as differences per mille (parts per thousand, o/oo) relative to an arbitrary standard such as standard mean ocean water (SMOW):

$$\delta o/oo = [(R - R_{standard})/R_{standard}] \times 1000$$

where R and $R_{standard}$ are the isotope ratios ($^{2}H/^{1}H$ or $^{18}0/^{16}0$) of the sample and the standard, respectively (Freeze and Cherry, 1979).

Owing to the difference in isotope mass, the various isotopic forms of water have slightly different vapor pressures and freezing points, which gives rise to differences in $^{18}0$ and ^{2}H concentrations in various stages of the hydrologic cycle. The process whereby the isotope content of a substance changes as a result of evaporation, condensation, freezing, melting, chemical reactions, or biological processes is known as isotopic fractionation. In most surface and shallow ground waters, fractionation is dependent only upon the processes of condensation and evaporation. When ocean water is evaporated, the vapor is depleted in $^{18}0$ and ^{2}H relative to the ocean water. Condensation of the water vapor produces rain or snow of relatively higher $^{18}0$ and ^{2}H than the initial vapor.

Concentrations of ^{2}H and $^{18}0$ obtained from global precipitation surveys correlate according to the relationship

$$\delta^{2}H = 8\delta^{18}0 + 10,$$

(Craig, 1961) which is known as the meteoric water line. The departure of $^{18}0$ and ^{2}H concentrations from the meteoric water line is a useful concept in a variety of hydrologic investigations. Of particular interest in this report is the effect of evaporation on infiltrated-water quality.

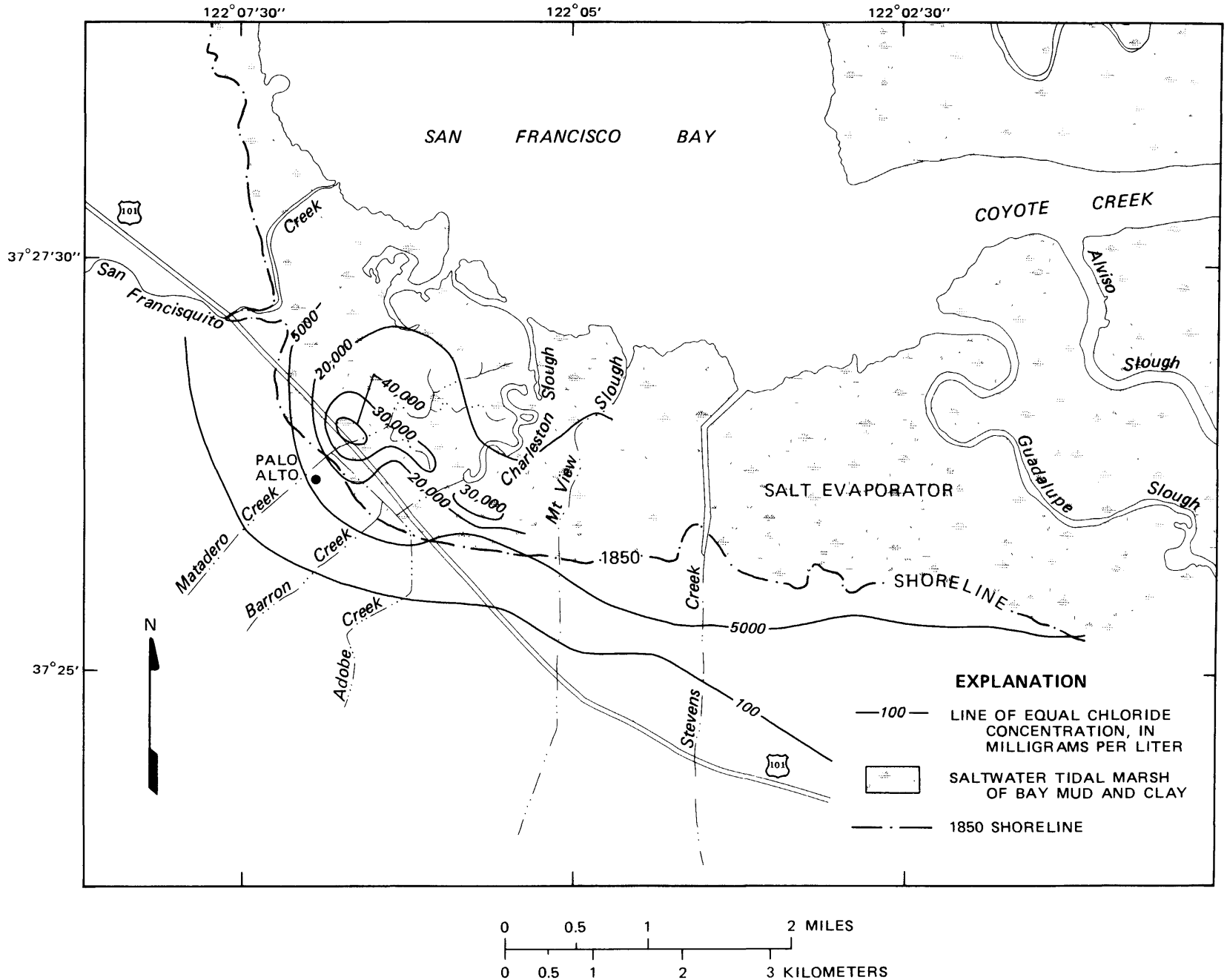

FIGURE 17. — Marsh distribution, present and 1850 shoreline, and chloride contours in the vicinity of the study area.

Stable isotope ratios of ground water may indicate evaporation or mixing. Because these processes can produce the same isotope ratios, additional chemical data must be used to differentiate between the two. Stable isotope ratios for hydrogen (δD) and oxygen ($\delta^{18}O$) have been determined from samples of ground water and local surface water, including bay, slough, creek, and pond water (Appendix B). Samples were taken at fifteen wells that were screened in the lower aquifer and six surface-water sites in the vicinity of injection well I6 (fig. 3). The regression equation

$$\delta D = 6.19\ \delta^{18}O - 7.50$$

was derived from and applied to the data as shown in figure 18. This regression line lies below and to the right of the meteoric water line,

$$\delta D = 8\ \delta^{18}O + 10$$

(Craig, 1961), which supports the conclusion that the ground water has been exposed to evaporative conditions. The ground-water isotope composition is bracketed by local freshwater and baywater compositions. A plot of chloride versus δD for ground water from the lower (45-foot) aquifer (fig. 19) may help to differentiate between simple mixing and evaporation as mechanisms for formation of the saline ground water. Most of the ground-water samples plot above standard mean ocean water and baywater in chloride concentration, which precludes the possibility of simple mixing.

CHEMICAL INTERACTIONS DURING INJECTION AT WELL I9

Injection Parameters and Sampling Techniques

Injection well I9 is located at the southern end of the well network on the levee bordering Charleston Slough (fig. 3). Variations of ground-water quality were monitored in observation wells U17 and U18, located 31 feet west and 51 feet east of well I9, respectively. These three wells were screened in the lower (45-foot) aquifer. Injection began on June 9, 1980, at 1000 hours. During June, 7.2 acre-ft of water were injected over a period of 22 days at an average injection rate of approximately 74 gal/min. During July, the final month of injection, 9.5 acre-ft of water were injected over a period of 31 days at an average rate of 70 gal/min.

Water samples were collected at wells U17 and U18 to examine the effects of injected freshwater upon local ground-water quality. Collection and treatment of samples for major ions (including alkalinity), trace metals, isotopes, and nutrients were done according to procedures described by Wood (1976). Before sample collection, stabilization of electrical conductivity was determined, and the 1-inch diameter PVC wells were purged of several casing volumes by means of an all-plastic bilge pump. Temperature, pH, and specific conductance were measured in the field according to techniques outlined by Presser and Barnes (1974). Tables 1, 2, and 3 show water-quality data from samples at wells U17, U18, and I9 (injection water) by date and time during the injection test.

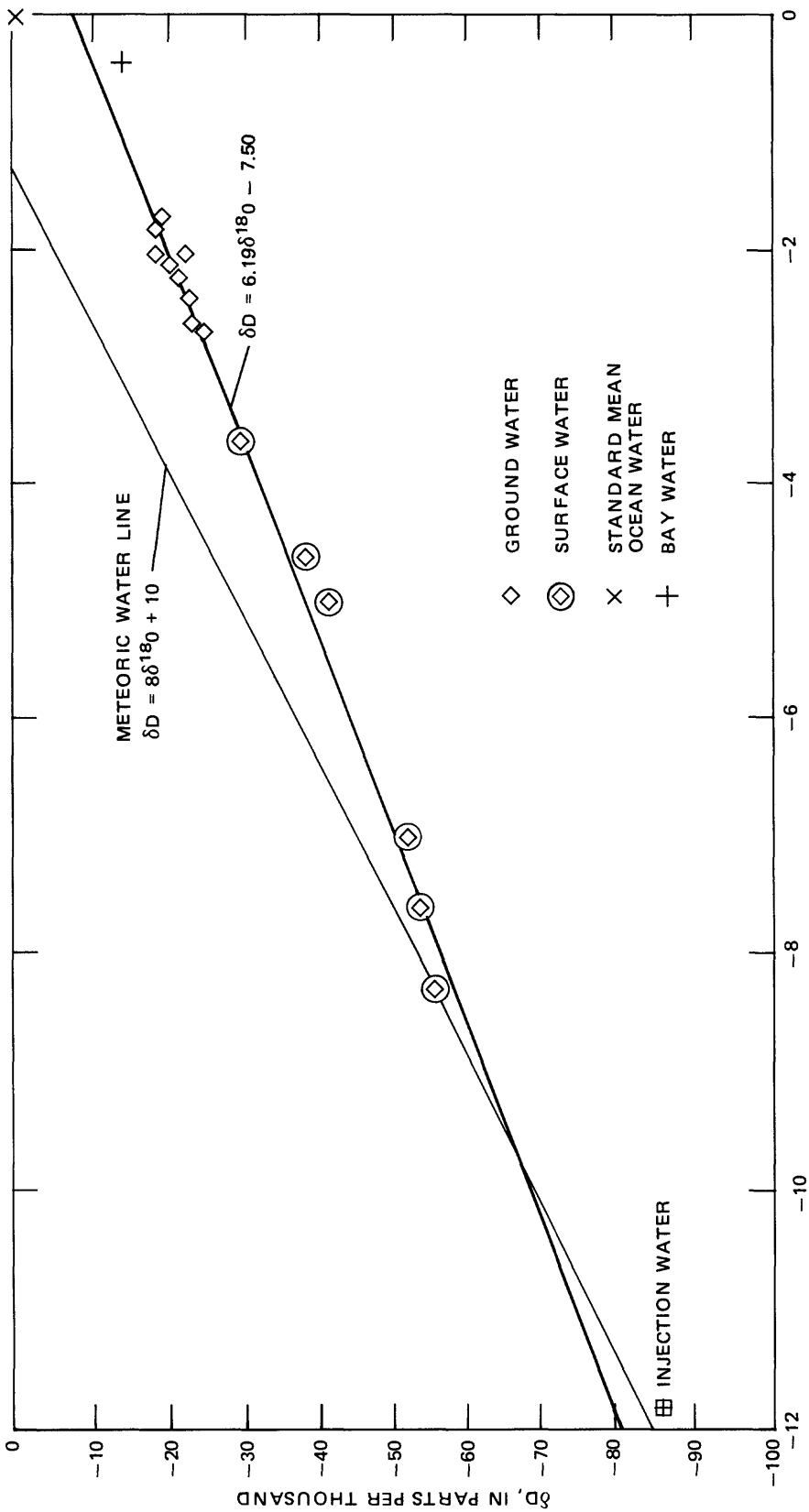

FIGURE 18. – Isotope ratios for hydrogen and oxygen in ground water, surface water, injection water, and standard mean ocean water. Plot of δD and $\delta^{18}O$ ratios for surface and ground-water samples fitted to the regression line $\delta D = 6.19\delta^{18}O - 7.50$ in relation to the meteoric water line.

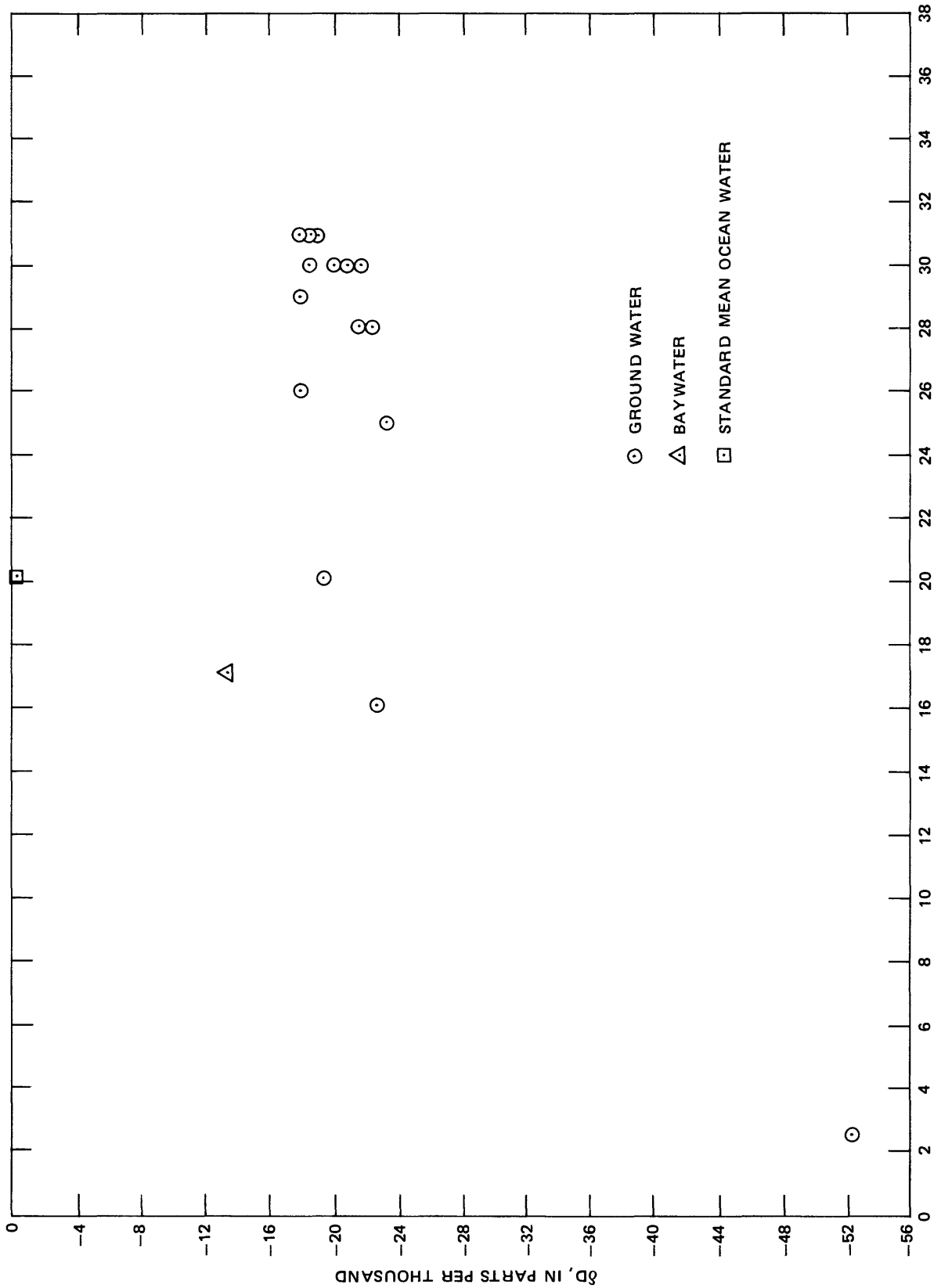

FIGURE 19. — Plot of chloride concentration versus δD for ground water, baywater, and standard mean ocean water.

TABLE 1.--Ground-water-quality data from samples at observation well U17 during injection at well I9

[Injection began June 9, 1980. All dates are in 1980. Temperature and pH were measured or determined on site. All data in milligrams per liter unless otherwise indicated]

Date	Time (hours)	Temperature (°C)	pH	Calcium	Magnesium	Sodium	Potassium	Chloride	Sulfate	Alkalinity	Silica	Boron (µg/L)	Fluoride	Manganese (µg/l)
June 5	1400	18.0	7.00	750	2,000	15,000	390.0	26,000	3,400	--	19	4,800	0.3	7,200
June 9	1045	18.0	7.00	760	2,000	15,000	350.0	27,000	2,200	600	16	3,300	0.4	7,000
June 9	1330	19.0	--	750	2,000	14,000	350.0	27,000	2,200	680	17	3,900	0.2	7,100
June 9	1530	18.0	6.90	770	1,900	15,000	360.0	27,000	2,000	590	23	5,200	0.2	7,400
June 9	1940	18.0	6.80	720	1,900	14,000	240.0	28,000	2,000	670	17	4,100	0.3	7,300
June 9	2330	17.0	7.00	600	1,500	12,000	290.0	21,000	2,500	610	17	4,700	0.4	5,400
June 10	0130	16.5	7.00	400	1,000	10,000	250.0	18,000	1,200	680	18	4,100	0.6	3,200
June 10	0340	15.5	7.10	310	830	9,000	210.0	15,000	1,800	650	17	4,700	0.6	2,800
June 10	0530	16.5	7.10	250	660	7,400	180.0	13,000	1,100	630	18	3,500	0.6	2,100
June 10	0720	17.0	7.20	220	550	6,800	160.0	12,000	1,300	550	18	5,100	0.6	1,700
June 10	1115	18.5	7.20	180	440	6,000	130.0	10,000	1,100	550	18	5,300	0.5	1,400
June 10	2230	17.0	7.30	88	240	4,000	92.0	6,200	880	440	38	2,800	0.3	770
June 11	1635	17.0	--	48	110	2,500	63.0	3,600	560	430	19	1,800	1.0	420
June 11	1945	18.0	7.50	46	110	2,300	58.0	3,700	320	350	19	1,800	1.0	400
June 12	1115	18.5	7.60	39	92	2,000	47.0	2,900	390	390	19	1,500	1.3	320
June 12	2015	18.0	6.95	35	79	1,700	46.0	2,400	420	350	18	1,500	1.4	290
June 13	1035	19.0	7.50	35	77	1,600	41.0	2,300	390	250	18	1,300	1.8	290
June 13	1630	19.0	7.45	37	77	1,600	40.0	2,200	370	300	18	1,200	1.9	300
June 14	0945	20.0	6.90	28	62	1,300	34.0	1,800	320	270	18	1,100	2.0	250
June 16	0945	20.0	7.05	23	44	1,000	26.0	1,400	260	170	17	850	2.3	170
June 23	1150	21.0	6.70	20	39	720	6.9	950	170	300	13	630	2.1	90
July 1	1245	21.0	6.70	24	39	640	24.0	800	160	220	13	720	2.0	120

TABLE 2.--Ground-water-quality data from samples at observation well U18 during injection at well I9

[Injection began June 9, 1980. All dates are in 1980. Temperature and pH were measured or determined on site. All data in milligrams per liter unless otherwise indicated]

Date	Time (hours)	Temperature (°C)	pH	Calcium	Magnesium	Sodium	Potassium	Chloride	Sulfate	Alkalinity	Silica	Boron (µg/L)	Fluoride	Manganese (µg/l)
June 5	1530	17.0	6.80	950	2,100	14,000	290.0	25,000	3,400	--	20	4,100	0.2	9,500
June 9	2200	17.0	6.90	980	2,000	14,000	270.0	27,000	2,400	560	17	4,300	0.3	9,100
June 10	0000	17.0	7.00	990	2,000	14,000	280.0	28,000	2,300	600	17	3,000	0.0	9,300
June 10	0200	16.5	7.00	870	2,000	14,000	280.0	27,000	6,200	430	17	--	0.0	8,900
June 10	0410	15.5	6.80	900	1,900	14,000	260.0	26,000	3,300	420	17	4,700	0.3	8,900
June 10	0600	16.5	6.80	890	1,900	14,000	250.0	26,000	3,100	580	17	2,700	0.2	8,700
June 10	0810	17.0	6.80	900	2,000	14,000	250.0	27,000	3,100	640	17	4,400	0.2	8,800
June 10	1145	18.0	6.90	910	2,000	14,000	270.0	26,000	3,100	510	17	3,600	0.1	9,200
June 10	2300	16.5	6.80	920	2,100	14,000	270.0	28,000	2,700	650	17	4,200	0.3	9,400
June 11	1715	17.0	--	730	1,700	12,000	220.0	23,000	3,800	480	20	4,500	0.2	7,100
June 11	2015	17.0	7.00	740	1,700	13,000	230.0	23,000	3,000	780	21	4,300	0.3	7,300
June 12	1240	18.0	7.10	380	850	8,000	150.0	13,000	2,000	700	20	4,700	0.5	3,300
June 12	2045	16.0	6.95	310	690	7,000	140.0	12,000	1,800	660	21	4,700	0.5	2,700
June 13	1320	18.0	6.50	190	440	5,600	100.0	9,100	1,300	540	20	4,400	0.9	1,800
June 13	1645	17.0	7.20	190	430	5,000	100.0	8,000	1,200	580	19	2,800	0.8	1,700
June 14	1010	16.5	6.80	130	330	4,000	180.0	6,300	1,200	590	21	2,300	0.6	1,300
June 16	1045	18.0	6.65	80	180	2,400	52.0	3,800	700	420	19	1,400	1.0	730
June 23	1235	19.5	6.60	9	23	820	19.0	1,000	260	300	17	1,200	2.6	100
July 01	1315	20.5	7.20	6	8	550	13.0	500	180	280	16	1,100	2.6	40
July 24	1400	22.0	6.20	95	150	1,200	31.0	2,100	300	240	11	950	1.9	590

TABLE 3.--Injection-water-quality data during injection at well I9

[Injection began June 9, 1980. All dates are in 1980. Temperature and pH were measured or determined on site. All data in milligrams per liter unless otherwised indicated]

Date	Time (hours)	Temperature (°C)	pH	Calcium	Magnesium	Sodium	Potassium	Chloride	Sulfate	Alkalinity	Silica	Boron (µg/L)	Fluoride	Manganese (µg/l)
June 9	1645	19.0	7.5	72	29	200	13	300	120	170	10	680	1.9	10
June 13	1615	20.0	11.2	130	0.5	170	13	240	110	280	4.4	680	2.1	<1
July 9	1440	22.2	6.1	96	6.9	160	13	230	100	130	3.8	470	2.0	9

Interpretation of Water-Quality Mixing Curves

Variations in the concentrations of dissolved constituents may be used to predict and determine chemical reactions that occur during injection. The types of behavior (enrichment, depletion, conservation) of dissolved constituents may be shown in plots of the various constituents versus chloride. The constituent of interest is plotted against the chloride ion relative to endpoints defined by the compositions of native and injection water. If one assumes that the chloride ion is conservative, the line connecting these endpoints indicates a nonreactive (conservative with respect to the aqueous phase) mixing path dependent only on physical interaction between solutions. Points along a smooth curve connecting the endpoints above the conservative-mixing line indicate reactions that release the constituent. Conversely, points that lie below the conservative-mixing line result from reactions that remove the constituent. Used with ion-ratio data and other chemical information, this method of analysis can help in understanding chemical changes that occur during injection of recycled water.

Sodium, Potassium, Calcium, and Magnesium

Sodium, potassium, calcium, and magnesium are apparently linked through ion-exchange reactions within exchangeable clays and organic compounds. Ion-exchange reactions can be represented by an equation of the form, as for sodium and calcium,

$$Ca^{2+} + Na_2X = CaX + 2Na^{+},$$

where X indicates an exchange site (Robson and Saulnier, 1981). Magnesium behaves similarly to calcium. Montmorillonite and illite provide exchangeable sites for these reactions. Calcium and magnesium--small, highly-charged cations--are held in the clay lattice in preference to large monovalent cations like sodium. Under saline ground-water conditions, sodium may dominate within the exchange sites. The ionic structure in the sodic-clay double layer results in excessive hydronium (H_3O^+) ionic coordination when the native solution is diluted, which causes swelling of the lattice and possibly dispersion of clay particles (McNeal and others, 1966).

If one assumes that 4.9 mmol/L of calcite were dissolved, 8.6 mmol/L of calcium were exchanged for Na^+, and 13.8 mmol/L of magnesium and 0.7 mmol/L of K^+ were taken up by exchange, releasing a total of 45.5 mmol/L of Na^+ to the aqueous phase, the mass-balance calculations for Ca, Mg, Na, K, and total carbon (calculated from pH and alkalinity) indicate that at well U17 on June 10, 1980, at 1115 hours, the sample contained 36.6 percent saline ground water and 63.4 percent injection water. There are probably other reactions affecting Na, K, Mg, and Ca. Possible sinks for Na are zeolites or feldspars similar to albite (L. N. Plummer, U.S. Geological Survey, written commun., 1982). The data indicate enrichment of sodium, but the magnitude of the apparent enrichment is less than that of the analytical-error limits, so that it cannot be quantified.

Ion exchange for sodium presumably removed calcium and magnesium from the water. The plot of these cations shows depletion from conservative mixing (figs. 20 and 21). Magnesium does not show depletion in the low-concentration range, which represents the completion of ground-water displacement by injection water. Exchange, therefore, occurs only during displacement of ground water by injection water. Calcium shows displacement over the entire range of concentrations, consistent with continuous ion-exchange reaction.

For a monovalent-divalent ion exchange, the thermodynamic equilibrium constant, K_{AB}, is equal to

$$\frac{[A^+]^2}{[B^{++}]} \quad \frac{[BX_2]}{[A_2X_2]}$$

(Garrels and Christ, 1965, p. 275). The relation for sodium-calcium exchange may be written

$$\frac{[Na^+]^2}{[Ca^{++}]} = K_{NaCa} \frac{[Na_2X_2]}{[CaX_2]}.$$

Values of log ($[Na^+]^2/[Ca^{++}]$) and log ($[Na^+]^2/[Mg^{++}]$) average about 1.6 ± 0.1 and 0.9 ± 0.1, respectively, for samples with 26,000 and 10,000 mg/L of Cl^- at well U17; the values then drop off systematically (L. N. Plummer, U.S. Geological Survey, written commun., 1982). The constant values for Na:K and Na:Ca ratios indicate that exchange reactions control the major cations. The drop in Na:Ca and Na:Mg values represents a shift from monovalent-divalent ion exchange to other possible controls, such as simple dilution and dissolution. Falling Na:Ca and Na:Mg ratios indicate that Na concentration is dropping more rapidly than Ca and Mg concentrations in the ground water. This condition is consistent with the greater contrast in Na concentration between ground and injection water than for Ca and Mg. The dropoff in Ca concentration may also be offset by dissolution of calcite during dilution, which releases Ca.

Alkalinity (as $CaCO_3$)

Alkalinity was significantly enriched, up to 200 mg/L, over the conservative mixing line (fig. 22). Calculations show that mixing small amounts of native ground water with the injection water causes undersaturation with respect to calcite (L. N. Plummer, U.S. Geological Survey, written, commun., 1982). Ion exchange (Ca^{++} for $2Na^+$) results in further undersaturation, which can cause $CaCO_3$ dissolution. Thus, thermodynamics favor $CaCO_3$ solution, resulting in an increase in CO_3^{2-} and HCO_3^- in alkalinity. X-ray diffraction analysis of aquifer material in native ground water revealed a small amount of calcite.

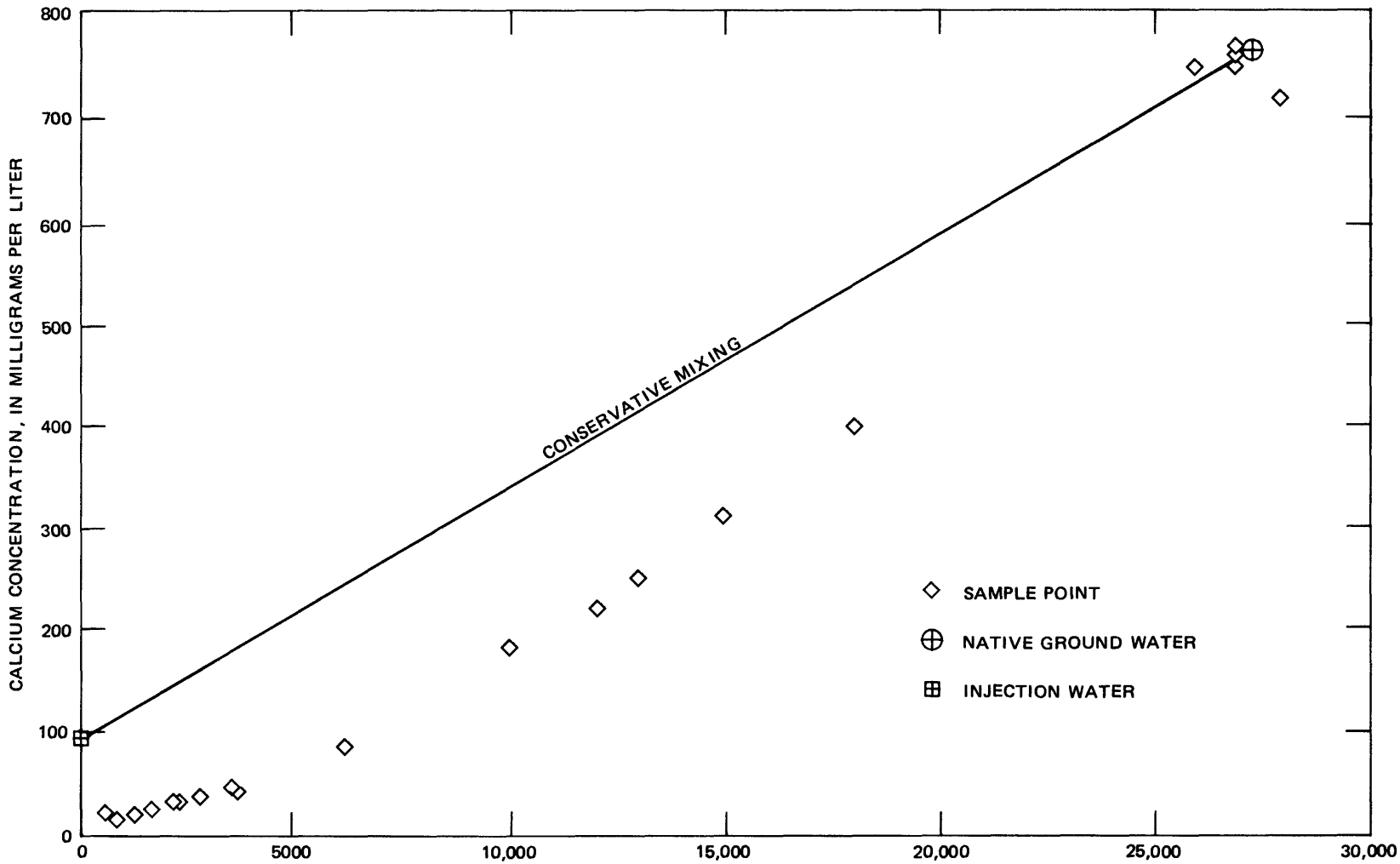

FIGURE 20. – Plot of calcium versus chloride concentration at well U17.

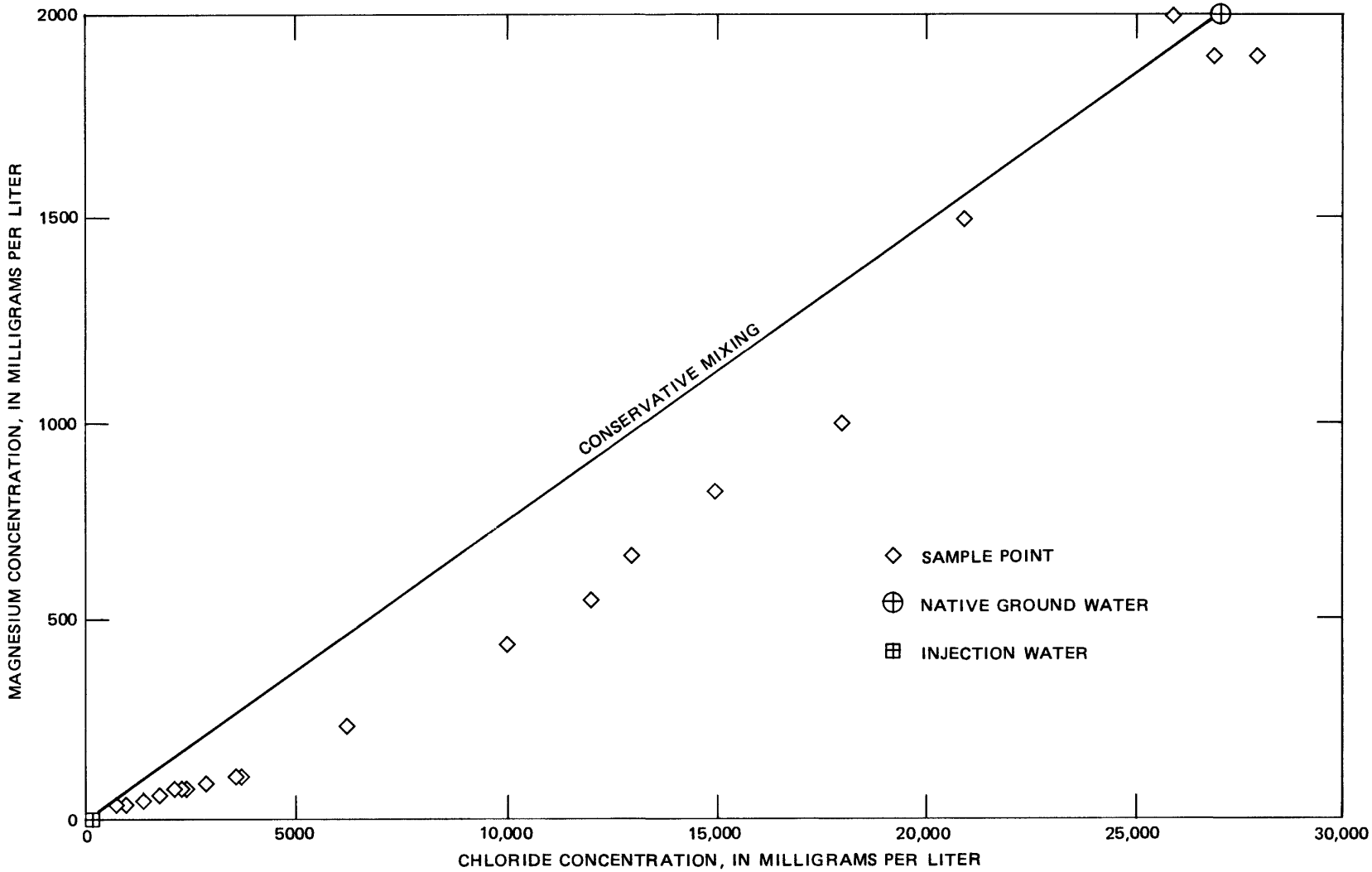

FIGURE 21. – Plot of magnesium versus chloride concentration at well U17.

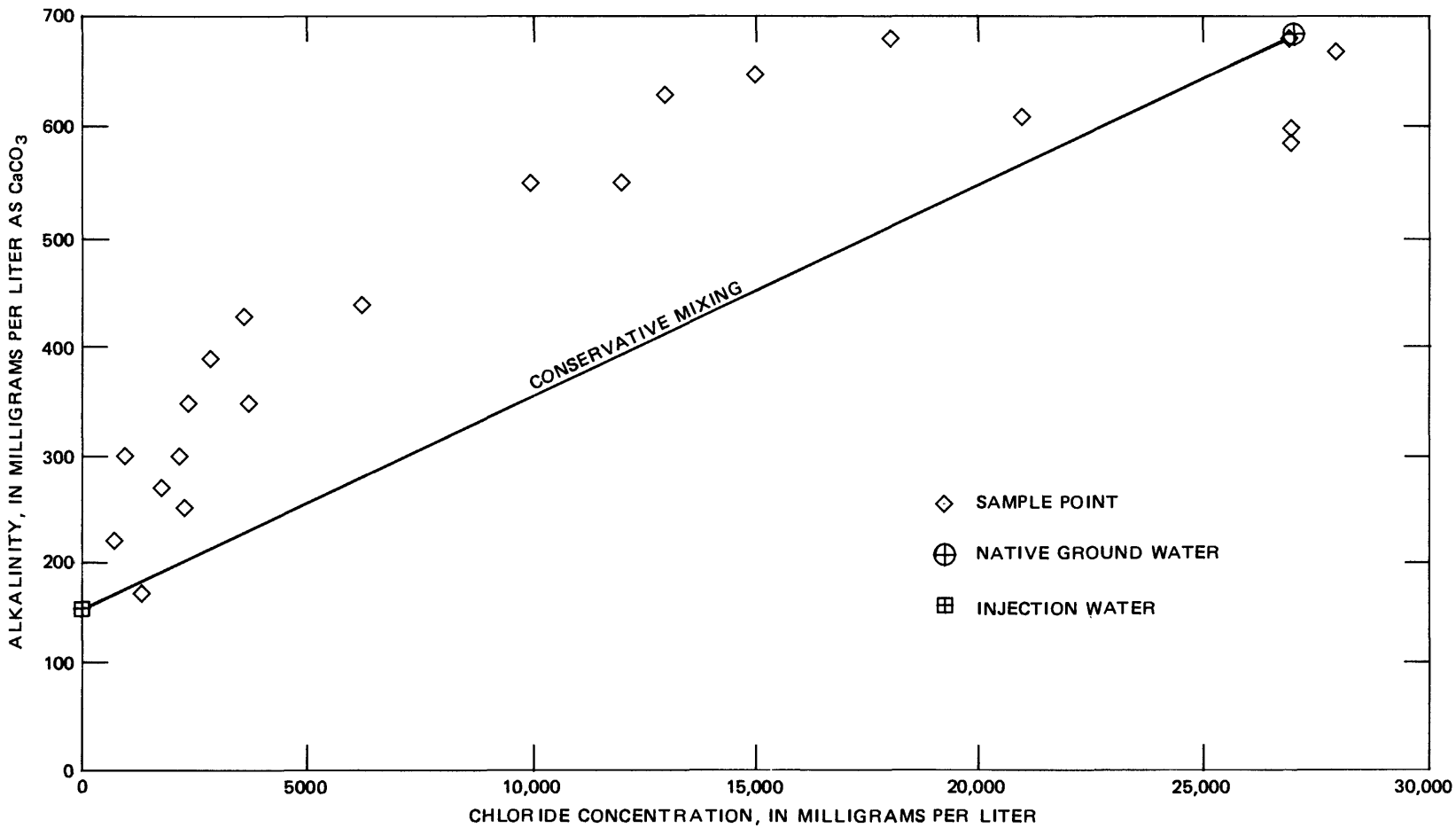

FIGURE 22. – Plot of alkalinity versus chloride concentration at well U17.

During sampling, pumping influenced pH of the ground-water sample, probably because of CO_2 evolution and subsequent decrease in total carbonate. Pertinent reactions are as follows:

$$H_2\ CO_{3_{aq}} = CO_2\ (aq) + H_2O \text{ and } H_2CO_{3_{aq}} = H^+ + HCO_3^-$$

(Stumm and Morgan, 1970). Total alkalinity (the sum of the bicarbonate, carbonate, and hydroxide alkalinity) is a conservative property of water that is not influenced by temperature, pressure, or addition or removal of carbon dioxide. Exchange of carbon dioxide, however, does influence the individual components. When carbon dioxide is lost, as in the present case, the pH increases and a stoichiometric amount of bicarbonate is converted to carbonate ion and hydroxide ion (Pagenkopf, 1978, p. 102). To avoid this effect, an in-site pH probe was used to measure ground-water pH.

Silica

Dissolved silica remained fairly constant between values expected for equilibrium with chalcedony (29 mg/L) and quartz (6.0 mg/L) at 25°C (fig. 23). Silica enrichment over the mixing line can result from dissolution of chalcedony or other silicate minerals (L. N. Plummer, U.S. Geological Survey, written commun., 1982). Chalcedony is common in sedimentary rocks. Other possible sources of dissolved silica include quartz, aluminosilicates, and ferrosilicates.

Manganese

The data indicate systematic depletion of manganese (fig. 24). Since most of the waters were undersaturated with $MnCO_3$, precipitation of manganese oxy-hydroxides and (or) adsorption may have provided a sink for manganese (L. N. Plummer, U.S. Geological Survey, written commun., 1982).

Boron

Boron shows enrichment over conservative mixing (fig. 25). Boron may occur in potassium feldspars of saline, alkaline, lacustrine deposits (Sheppard and Gude, 1973). The marsh environment supplies conditions necessary for formation of these minerals. Dissolution of such clays as illite may also release boron (L. N. Plummer, U.S. Geological Survey, written commun., 1982). Boron concentration was quite high, about 4 mg/L, in the native ground water. Concentration in the treated wastewater used for injection was about 0.6 mg/L, so that injection lowered the concentration of boron in the ground water. Inasmuch as the aqueous chemistry of boron is intricate and not well understood, the actual solute species present in the Palo Alto ground water are not known.

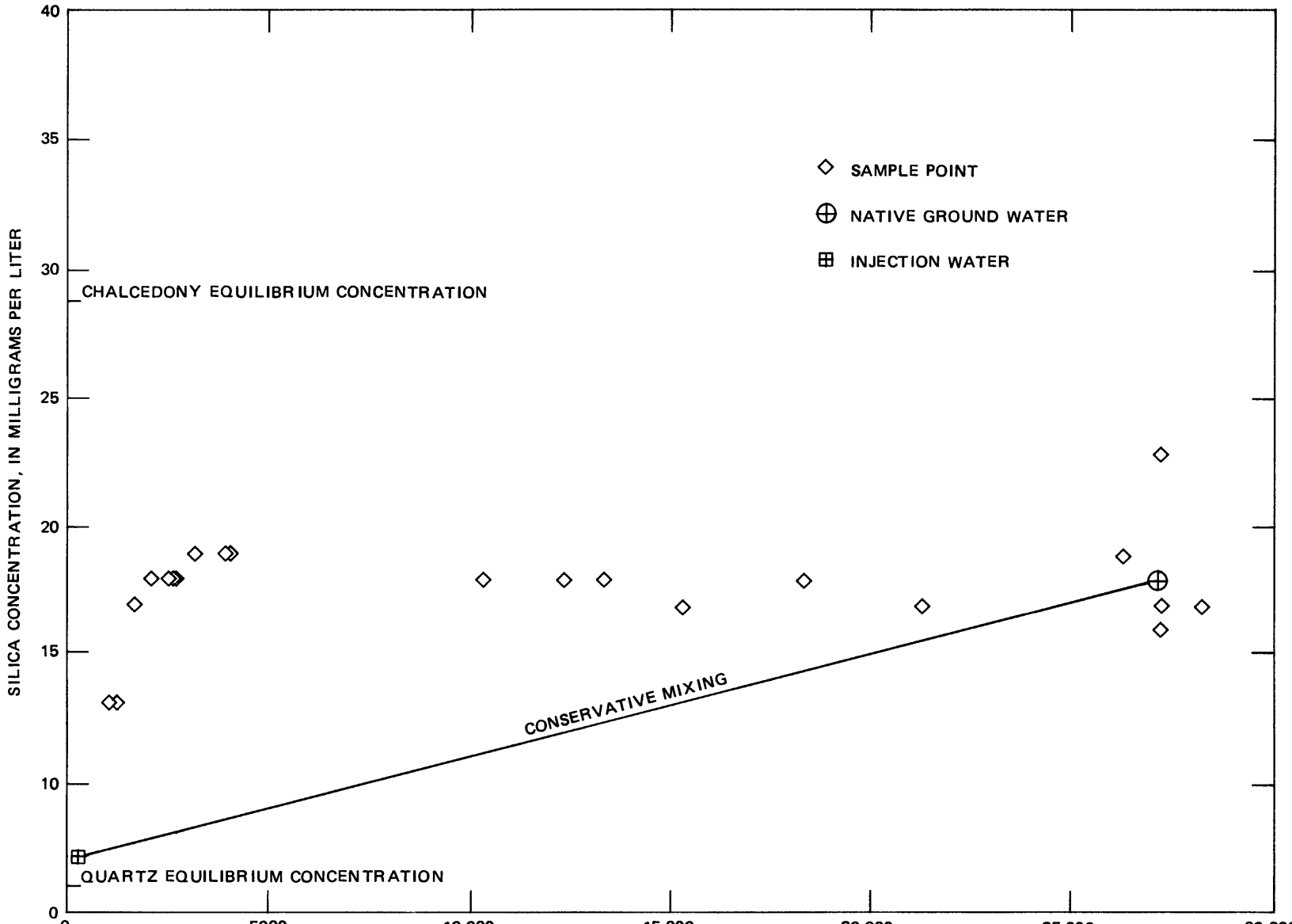

FIGURE 23. – Plot of silica versus chloride concentration at well U17.

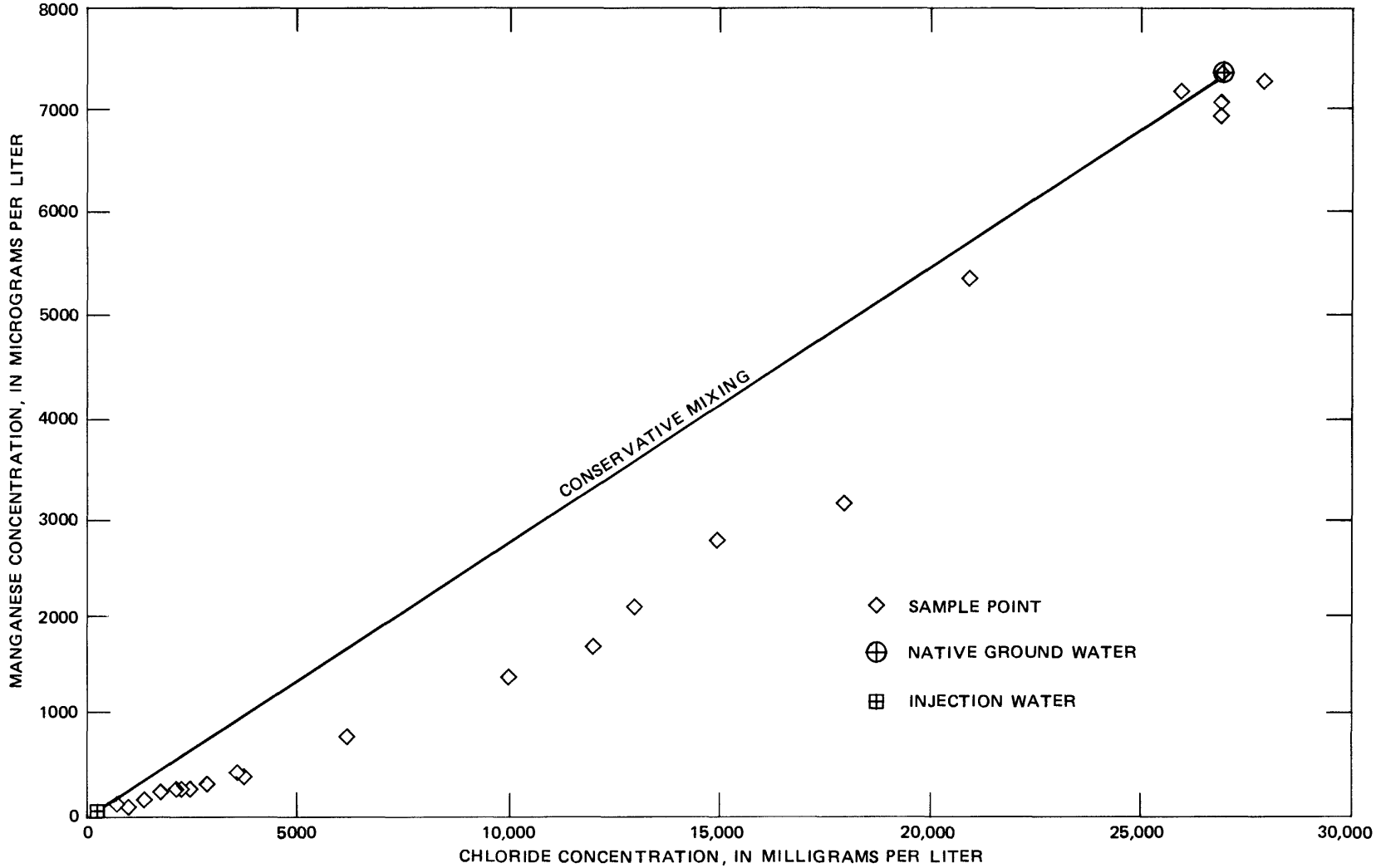

FIGURE 24. – Plot of manganese versus chloride concentration at well U17.

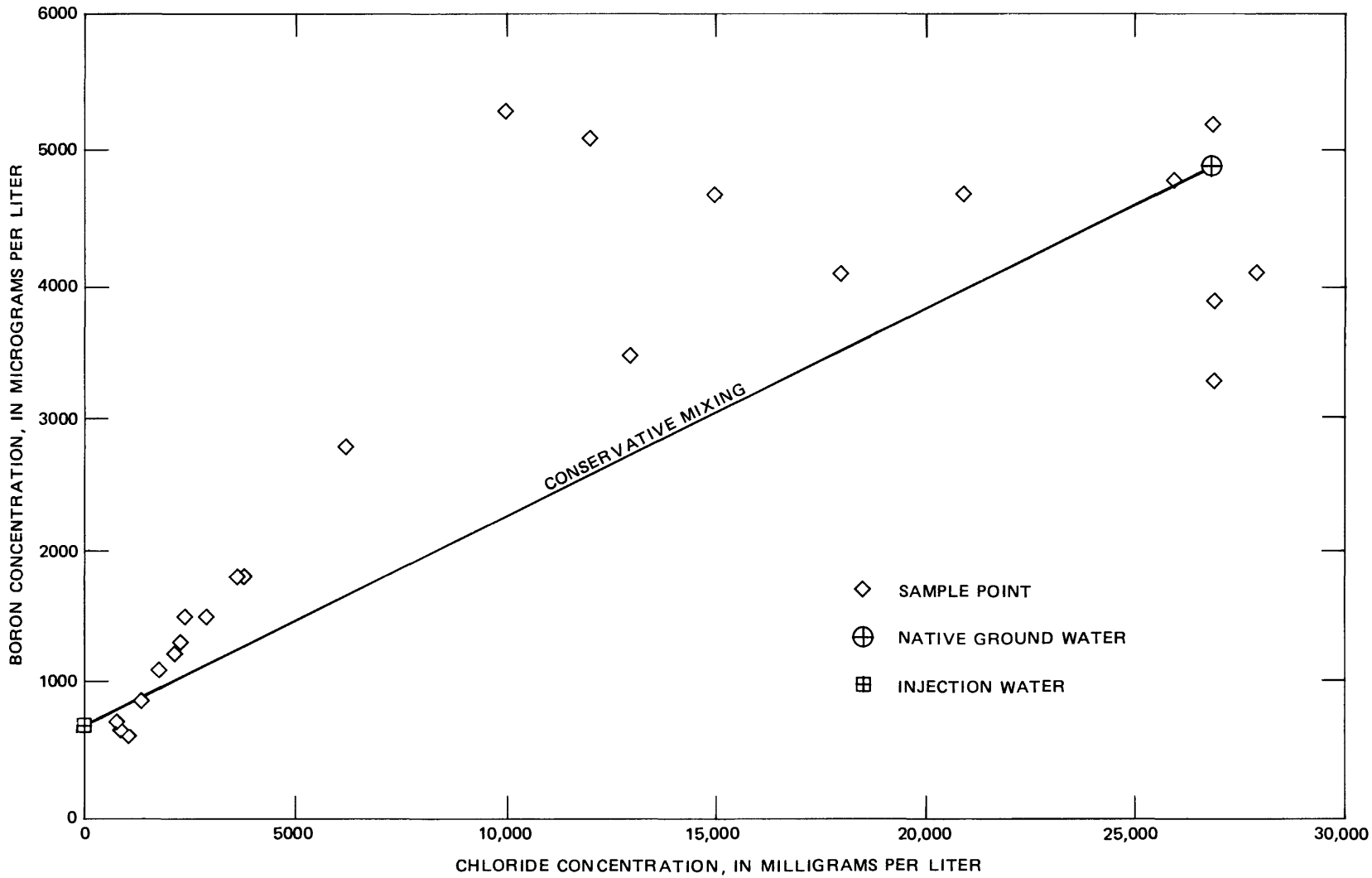

FIGURE 25. – Plot of boron versus chloride concentration at well U17.

Fluoride

Most of the fluoride data fall below the conservative-mixing line, indicating depletion (fig. 26). Speciation calculations show that the water was undersaturated with respect to fluorite (L. N. Plummer, U.S. Geological Survey, written commun., 1982). Fluoride ions have the same charge and nearly the same radius as hydroxide ions, so that the ions may tend to replace each other (Hem, 1970). Therefore, anion exchange may also have been involved in the depletion of fluoride during mixing. Fluoride data after breakthrough show a slight enrichment over conservative mixing, which may have resulted either from dissolution of fluoride compounds or from anion exchange.

Trace Elements

Concentrations of arsenic, cadmium, copper, and silver in ground water and injected water are shown in table 4. The paucity of data on these elements limits analysis to general discussion of their chemical behavior. Silver was not detected (detection limit is 1 µg/L) in the ground-water samples and therefore is not discussed. Within the constraints of chemical analysis, arsenic values remained fairly constant during injection. All determined values are well within safe drinking water standards (U.S. Environmental Protection Agency, 1977). The sorption of arsenate on precipitated ferric hydroxide or other active surfaces is probably an important factor limiting arsenic solubility in natural water systems (Hem, 1970). Cadmium values were at or below the detection limit before the test and below the range for injection water during the test. Cadmium was therefore removed from the injection water during passage through the aquifer. Low concentrations may have been caused by adsorption on clay minerals, hydrous oxides of iron and manganese, or organic matter. Isomorphous substitution or coprecipitation with minerals or amorphous solids may also have been important (Freeze and Cherry, 1979).

Copper also was removed from the injection water during its passage through the ground-water system. Values for mixed ground-water samples remained below those of injection water even after nearly complete breakthrough. Eh-pH diagrams given by Garrels and Christ (1965) suggest that cupric oxide and hydroxy-carbonate minerals tend to limit the solubility of copper in aerated (injection) water at a pH of 7.0 to about 10^{-6} mol/L (64 µg/L). The solubility is one-tenth as great, about 6.4 µg/L, at a pH of 8.0. During injection, observed values ranged from 8 to 18 µg/L (within a ground water pH range of 7.0 to 8.0). Concentration of copper in the injection water ranged from 15 and 50 µg/L.

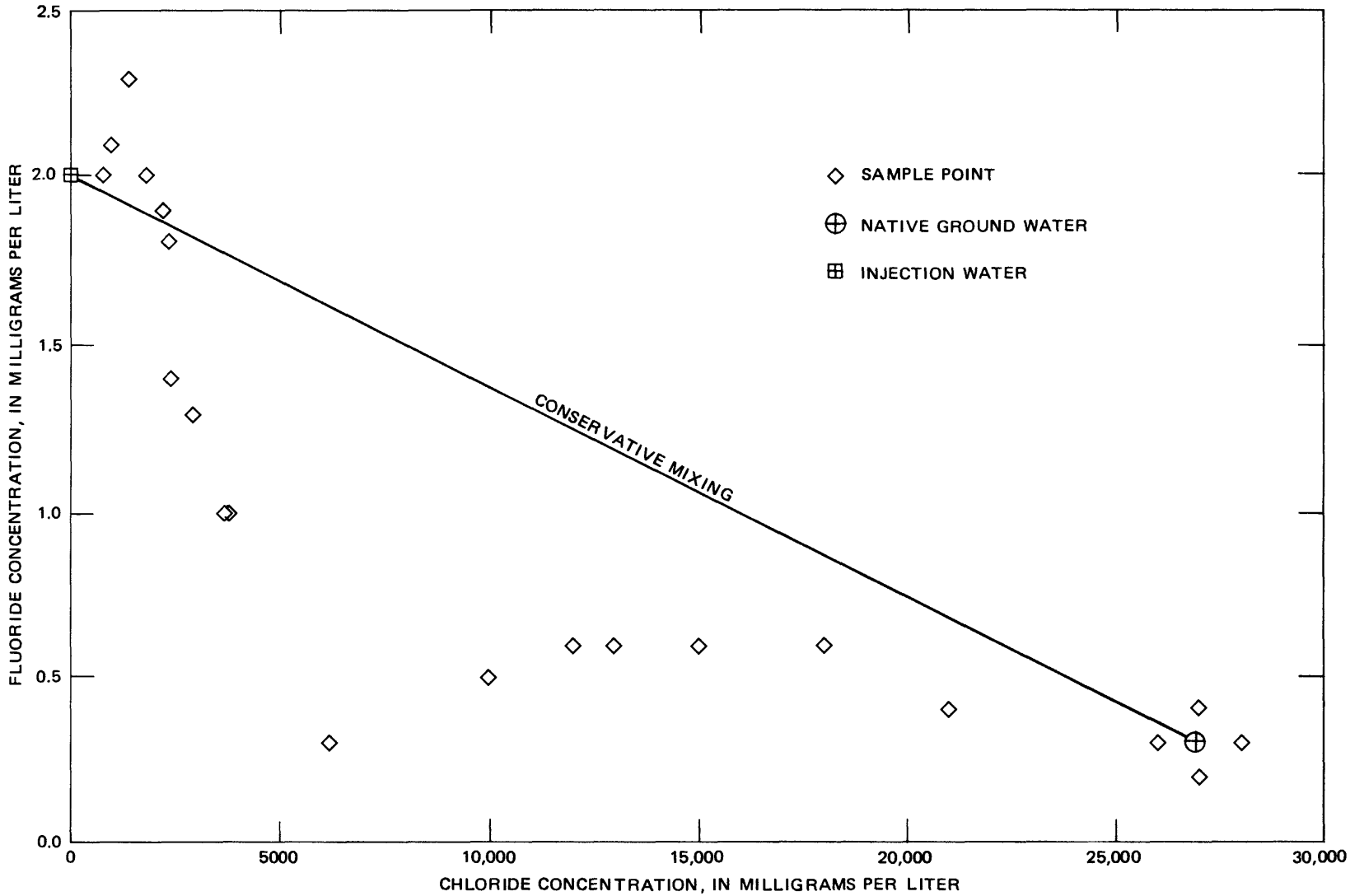

FIGURE 26. — Plot of fluoride versus chloride concentration at well U17.

TABLE 4.--Trace elements in ground water, injection water, and safe drinking water

[Injection began June 9, 1980; all dates are in 1980. Concentrations are given in micrograms per liter]

Well	Sample date	Arsenic	Cadmium	Copper	Silver
U17	June 6	4	1	14	<1
(ground water)	June 9	2	1	8	<1
	June 10	2	1	9	<1
	June 13	2	1	17	<1
	June 23	3	1	12	<1
	July 1	3	<1	11	<1
U18	June 5	3	1	14	<1
(ground water)	June 13	3	<1	10	<1
	June 23	4	1	12	<1
	July 1	7	<1	18	<1
	July 24	8	<1	9	<1
I9	June 9	4	5	15	<1
(injection	June 13	1	1	50	1
water)	July 9	1	2	23	<1
Safe drinking water[1]		50	10	100	50

[1]U.S. Environmental Protection Agency (1977).

SUMMARY OF FACTORS AFFECTING GROUND-WATER RECHARGE BY INJECTION

The performance of the injection-extraction well field is controlled by the geologic framework, hydraulic characteristics of the aquifer system, and chemical compatibility of ground and injection water. The efficiency of the system is inherently limited by well-field design, construction, and operation under the constraints of the natural environment. Efficient operation of the well field may be attained by modifying the variables of extraction (quantity and distribution) and injection (quantity, distribution, and water quality) to complement the ground-water system.

The geologic framework and hydraulic gradient provide primary control over the migration paths of the injected water. In general, the structure and distribution of the aquifer system is complex and heterogeneous. The aquifer composition varies horizontally, reflecting transition between levee and channel deposits in a braided-stream depositional environment. Streams in the marsh form natural levees where silts and clays are distributed in bank deposits (Helley and La Joie, 1979). Drilling logs have defined a buried stream channel, which runs northwest to southeast through the study area. Particle-size analyses defined this channel as a bed of coarse material bounded by finer bank and levee deposits. Injection well I6 is located along the central axis of this ancient stream channel. Injected water preferentially follows a path through these highly permeable, coarse channel deposits.

Similarly, variations in the properties of the aquifer system and hydraulic gradient control the rate and direction of ground-water flow. The horizontal permeability in the lower aquifer (120 ft/d) is much greater than the vertical permeability in the confining clay layer (0.08 ft/d). Flow is therefore primarily horizontal and to a small degree vertical through the clay layer in proportion to the hydraulic gradient across this layer. This gradient increases as a result of injection, particularly near the injection well, and flow increases through the clay layer to the overlying aquifer. The initial response in the upper aquifer is an increase in salinity as saline water is apparently forced up and out of the intermediate clay. As freshwater penetrates the clay, salinity gradually drops in the upper aquifer. Vertical permeability may be reduced by swelling and dispersion in the clay layer induced by the freshwater. Dilution and replacement of saline ground water in the upper aquifer by vertical migration of injection water raises the water table in response to decreased fluid density under constant pressure. This effect was observed in the upper aquifer during injection to the lower aquifer near well I6.

Chemical interactions that may affect injection performance include precipitation, dissolution, and ion-exchange reactions. Precipitation of minerals, which can reduce or limit permeability, was neither observed during injection nor predicted by the mixing curves. On the other hand, there was evidence of dissolution of calcite in the aquifer as a result of dilution of native water by injected freshwater. This observation is supported by an apparent increase in specific capacity of the well during injection. Ion-exchange reactions, such as Ca^{+2} for Na^{+}, are likely in the clay layer. Substitution of calcium for sodium in the clay lattice reduces the magnitude of swelling and dispersion. However, replacement of saline ground water by fresh injected water causes expansion and possibly dispersion of sodic clay layers. This effect, which was observed in X-ray diffraction analysis of clay samples that had been soaked in both native and injected water, primarily affects clay-layer permeability, since the aquifer contains a relatively small amount of clay minerals.

REFERENCES CITED

Brown and Caldwell, Consulting Engineers, 1974, Geohydrologic investigation of the bayfront area, Palo Alto, California: Pasadena, Calif., 40 p.

Craig, Harmon, 1961, Isotope variations in meteoric waters: Science, v. 133, no. 3465, p. 1702-1703.

Freeze, R. A., and Cherry, J. A., 1979, Groundwater: Englewood Cliffs, N. J., Prentice-Hall, 604 p.

Garrels, R. M., and Christ, C. L., 1965, Solutions, minerals and equilibrium: New York, Harper and Row, 450 p.

Hamlin, S. N., 1983, Injection of treated wastewater for ground-water recharge in the Palo Alto baylands, California: Hydraulic and chemical interactions--preliminary report: U.S. Geological Survey Water-Resources Investigations Report 82-4121, 50 p.

Hantush, M. S., 1960, Modification of the theory of leaky aquifers: Journal of Geophysical Research, v. 65, no. 11, p. 3713-3725.

Helley, E. J., and La Joie, K. R., 1979, Flatland deposits--their geology and engineering properties and their importance to comprehensive planning: U.S. Geological Survey Professional Paper 943, 88 p.

Hem, J. D., 1970, Study and interpretation of the chemical characteristics of natural water: U.S. Geological Survey Water-Supply Paper 1473, 363 p.

Iwamura, T. I., 1980, Saltwater intrusion investigation in the Santa Clara County baylands area, California: Santa Clara Valley Water District Report, 115 p.

Jenks and Adamson, Consulting Sanitary and Civil Engineers, 1973, A program for water reclamation and ground-water recharge serving the Palo Alto bayfront area: Palo Alto, Project Report and Environmental Impact Statement, 150 p.

McNeal, B. L., and others, 1966, Effect of solution composition on the swelling of extracted soil clays: Soil Scientific Society of America, Proceedings, v. 30, p. 313-317.

Pagenkopf, G. K., 1978, Introduction to natural water chemistry: New York, Marcel Dekker, 272 p.

Presser, T. S., and Barnes, Ivan, 1974, Special techniques for determining chemical properties of geothermal water: U.S. Geological Survey Water-Resources Investigations Report 22-74, 11 p.

Roberts, P. V., and others, 1978, Groundwater recharge by injection of reclaimed water in Palo Alto: Palo Alto, Calif., Stanford University Civil Engineering Technical Report 225, 95 p.

Robson, S. G., and Saulnier, G. J., Jr., 1981, Hydrogeochemistry and simulated solute transport, Piceance Basin, Northwestern Colorado: U.S. Geological Survey Professional Paper 1196, 65 p.

Sheppard, R. A., and Gude, A. J., III, 1973, Boron-bearing potassium feldspar of authigenic origin in closed-basin deposits: U.S. Geological Survey Journal of Research, v. 1, no. 4, p. 377-382.

Stumm, Werner, and Morgan, J. J., 1970, Aquatic chemistry, an introduction emphasizing chemical equilibrium in natural waters: New York, Wiley-Interscience, 583 p.

Theis, C. V., 1935, The relation between the lowering of the piezometric surface and the rate and duration of discharge of a well using ground-water storage: Transactions of the American Geophysical Union, v. 16, p. 519-524.

Todd, D. K., 1980, Ground-water hydrology: New York, John Wiley, 535 p.

U.S. Environmental Protection Agency, 1977, National interim primary drinking water regulations: U.S. Environmental Protection Agency, Office of Water Supply, EPA-570/9-76-003, 159 p.

Valocchi, A. J., and others, 1981, Simulation of the transport of ion-exchanging solutes using laboratory-determined chemical parameter values: Groundwater, v. 19, no. 6, p. 600-607.

Wood, W. W., 1976, Guidelines for collection and field analysis of ground-water samples for selected unstable constituents: U.S. Geological Survey Techniques of Water-Resources Investigations, Book 1, Chapter D2, 24 p.

APPENDIXES

APPENDIX A.--Water-level and chloride data from observation wells

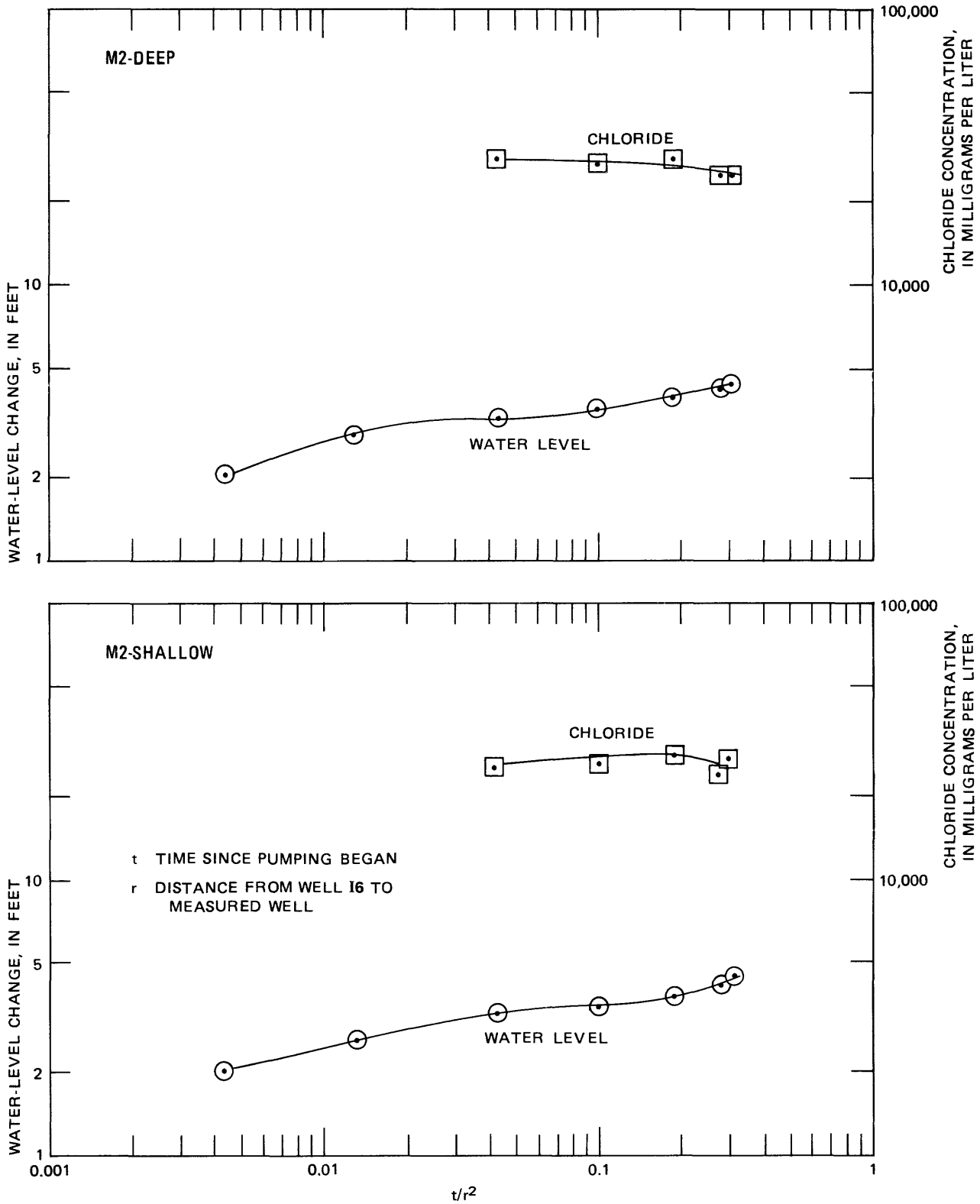

WATER-LEVEL AND CHLORIDE DATA AT WELL M2

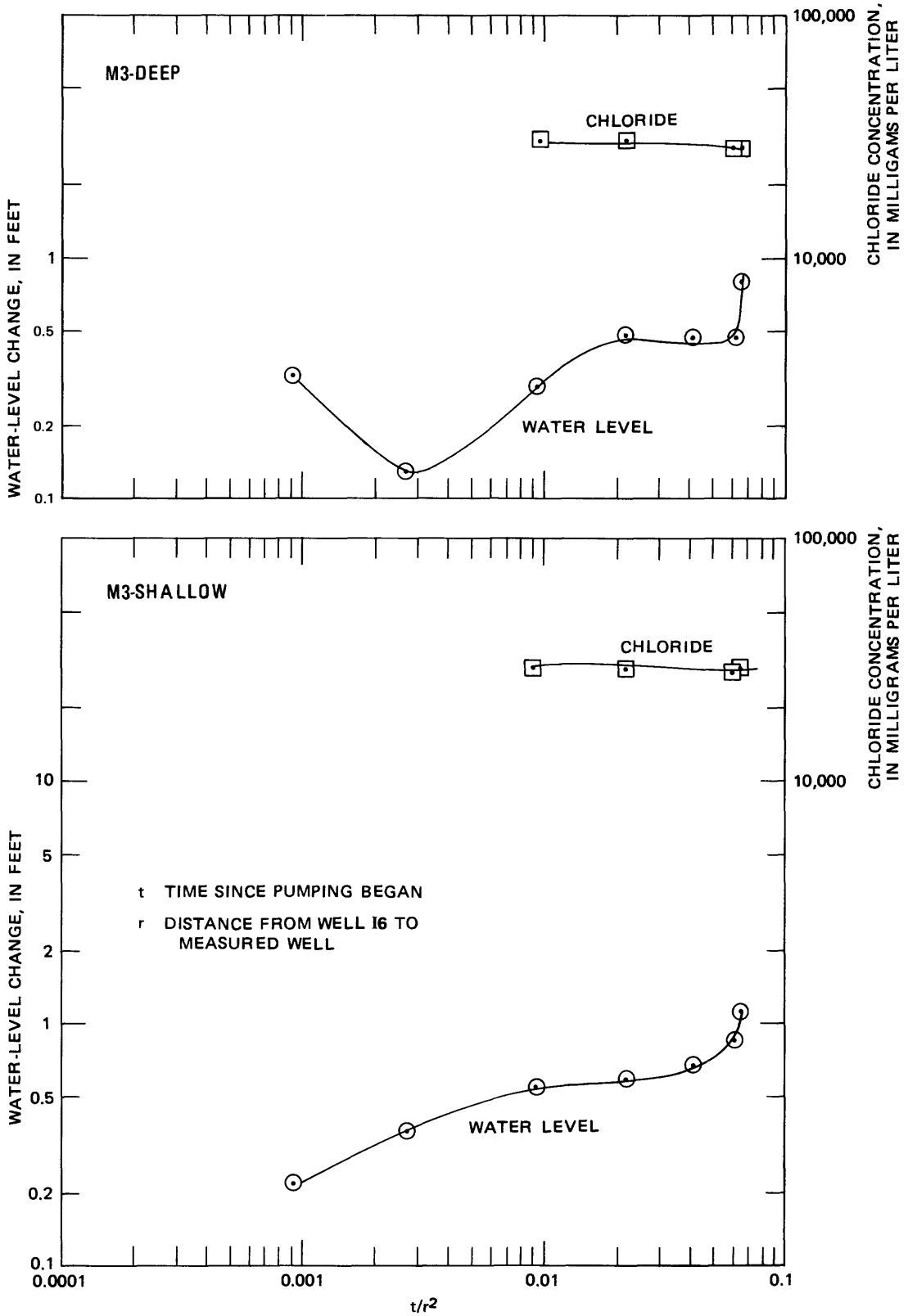

WATER-LEVEL AND CHLORIDE DATA AT WELL M3

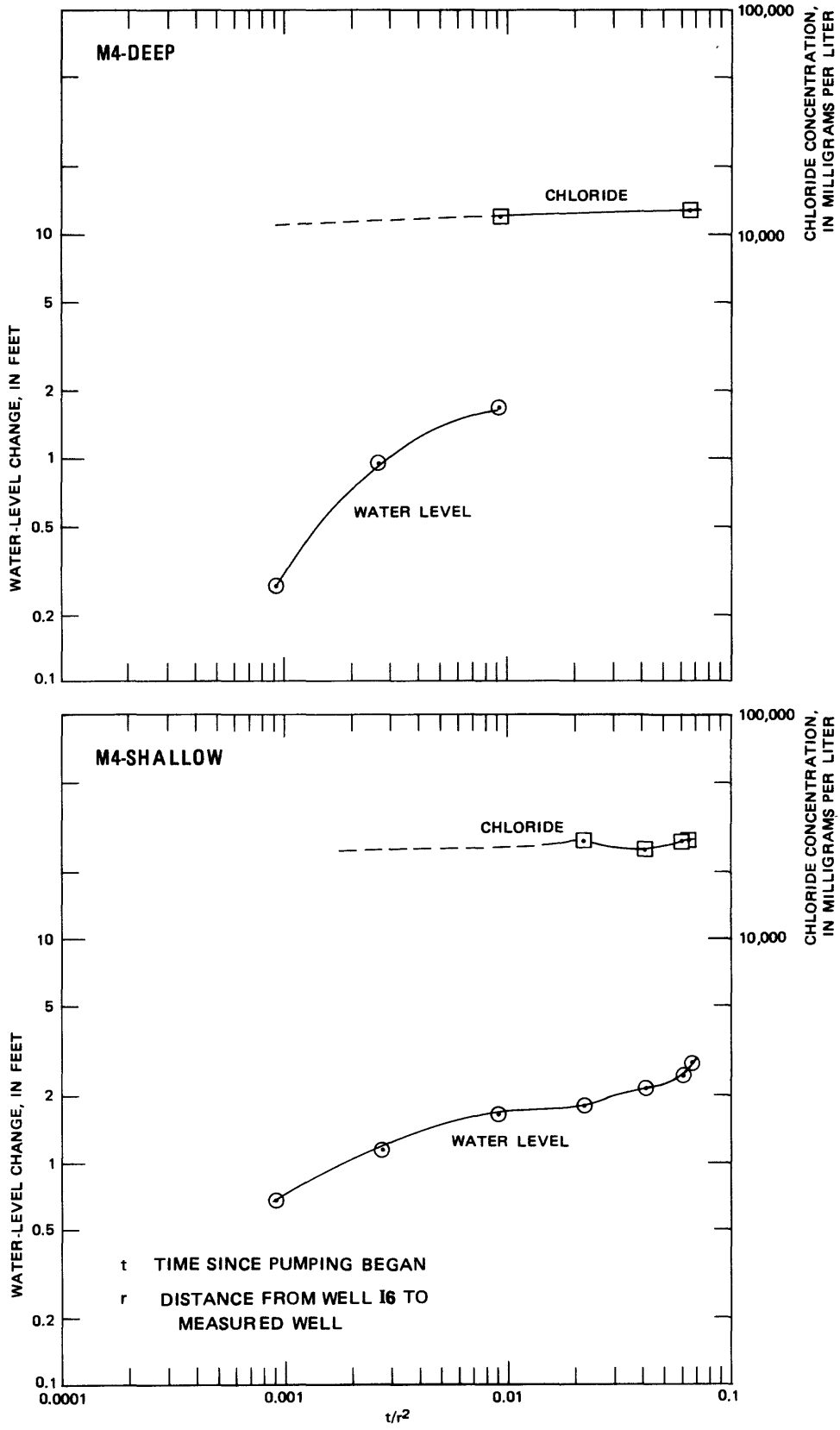

WATER-LEVEL AND CHLORIDE DATA AT WELL M4

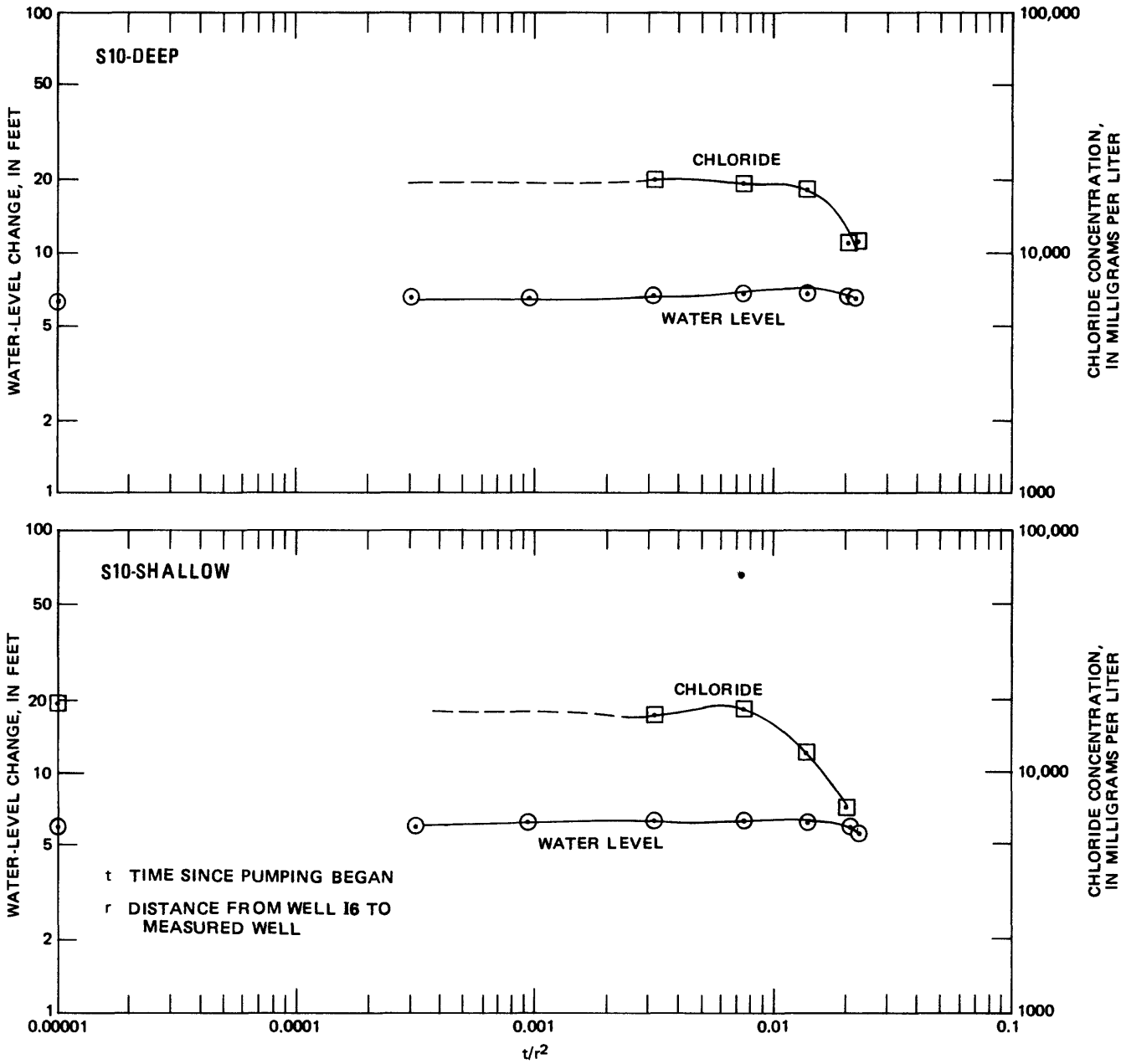

WATER-LEVEL AND CHLORIDE DATA AT WELL S10

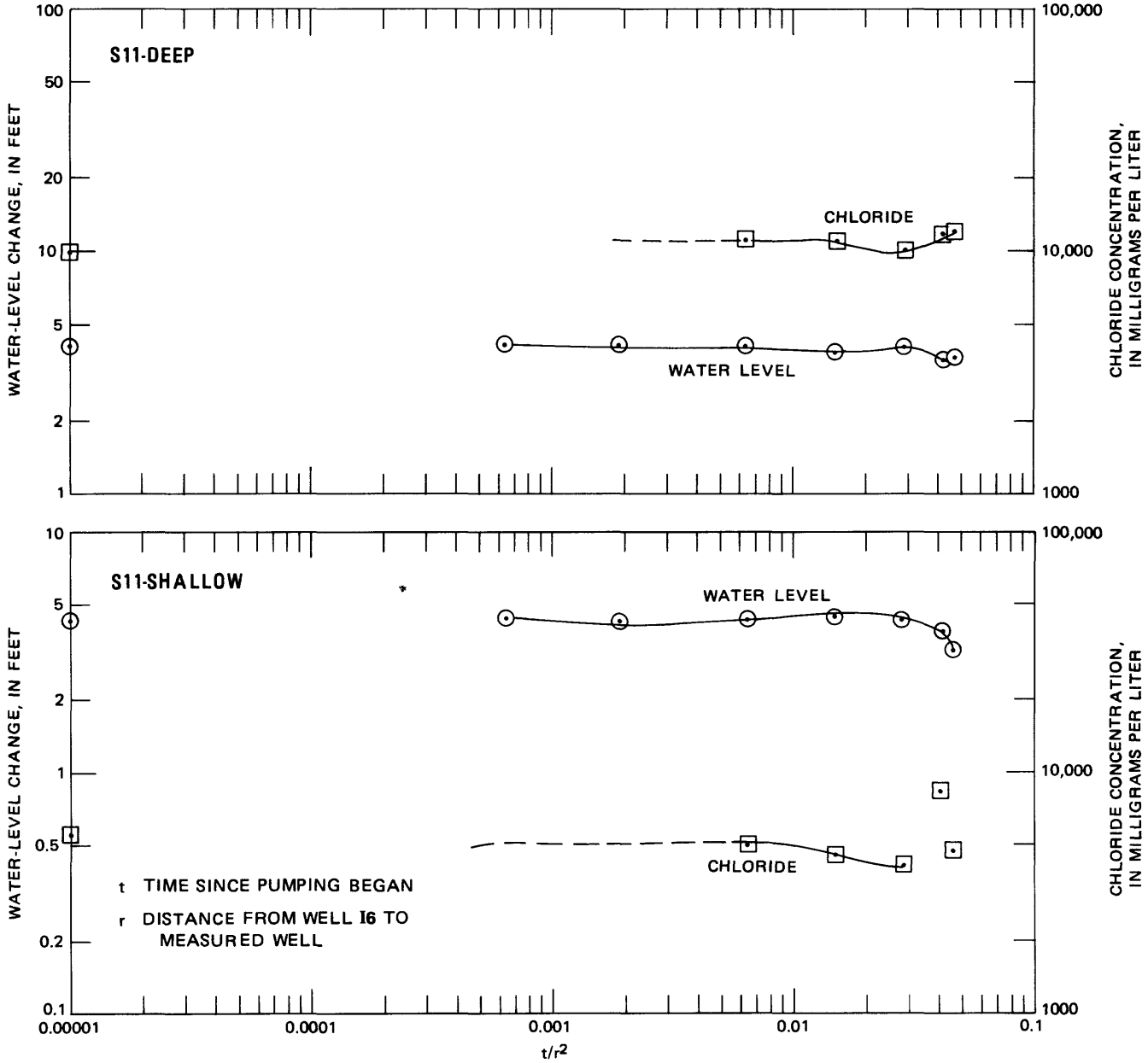

WATER-LEVEL AND CHLORIDE DATA AT WELL S11

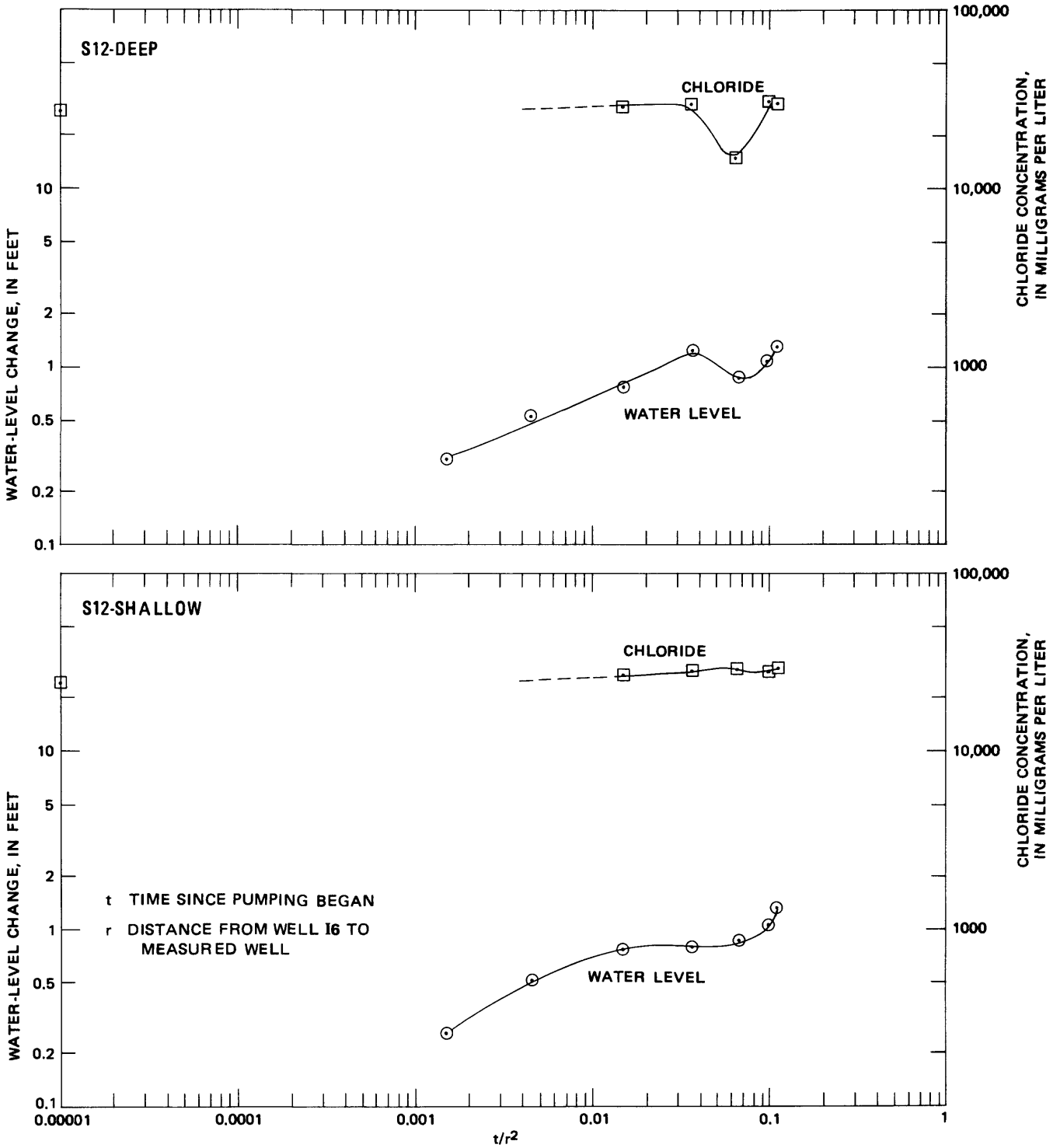

WATER-LEVEL AND CHLORIDE DATA AT WELL S12

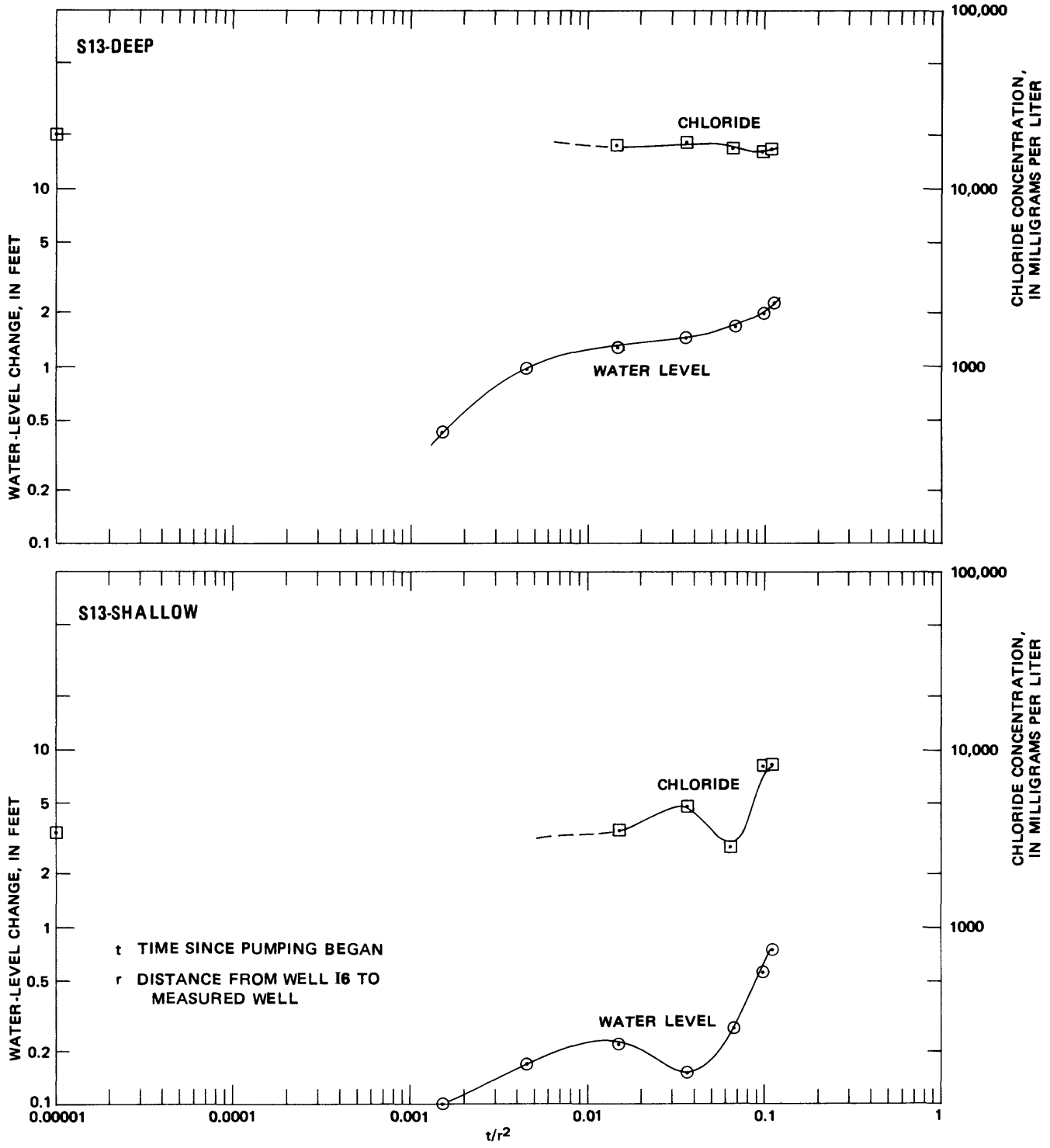

WATER-LEVEL AND CHLORIDE DATA AT WELL S13

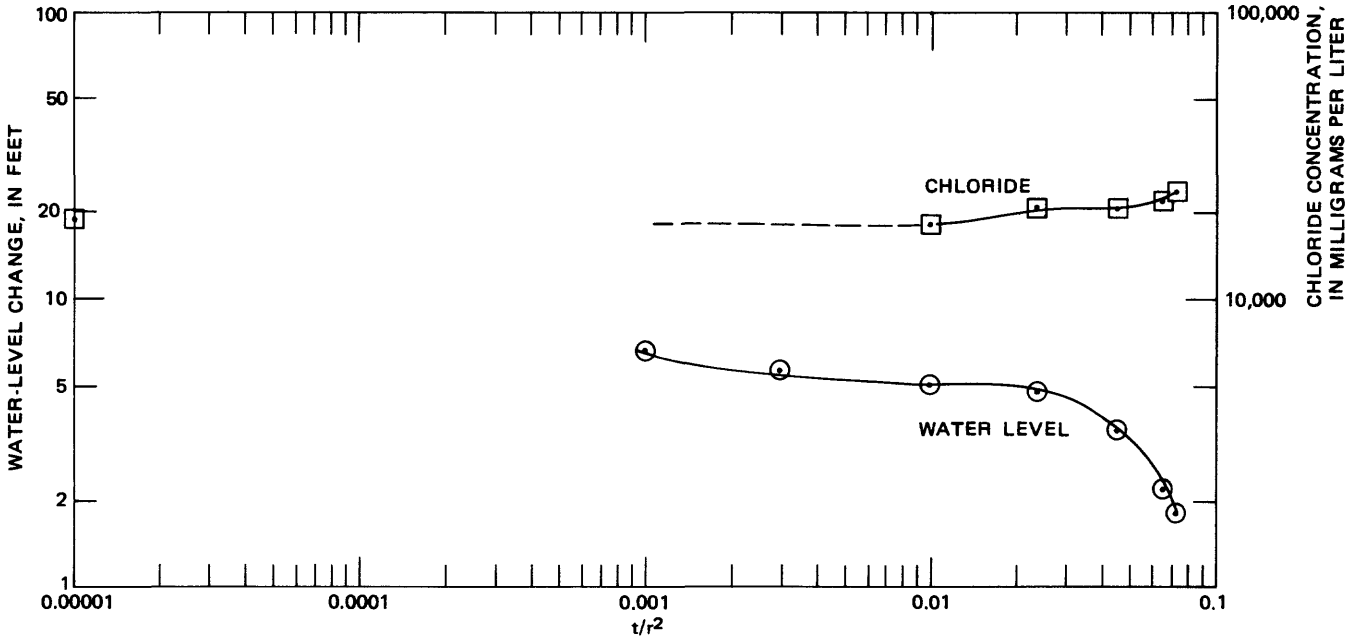

WATER-LEVEL AND CHLORIDE DATA AT WELL S15-DEEP

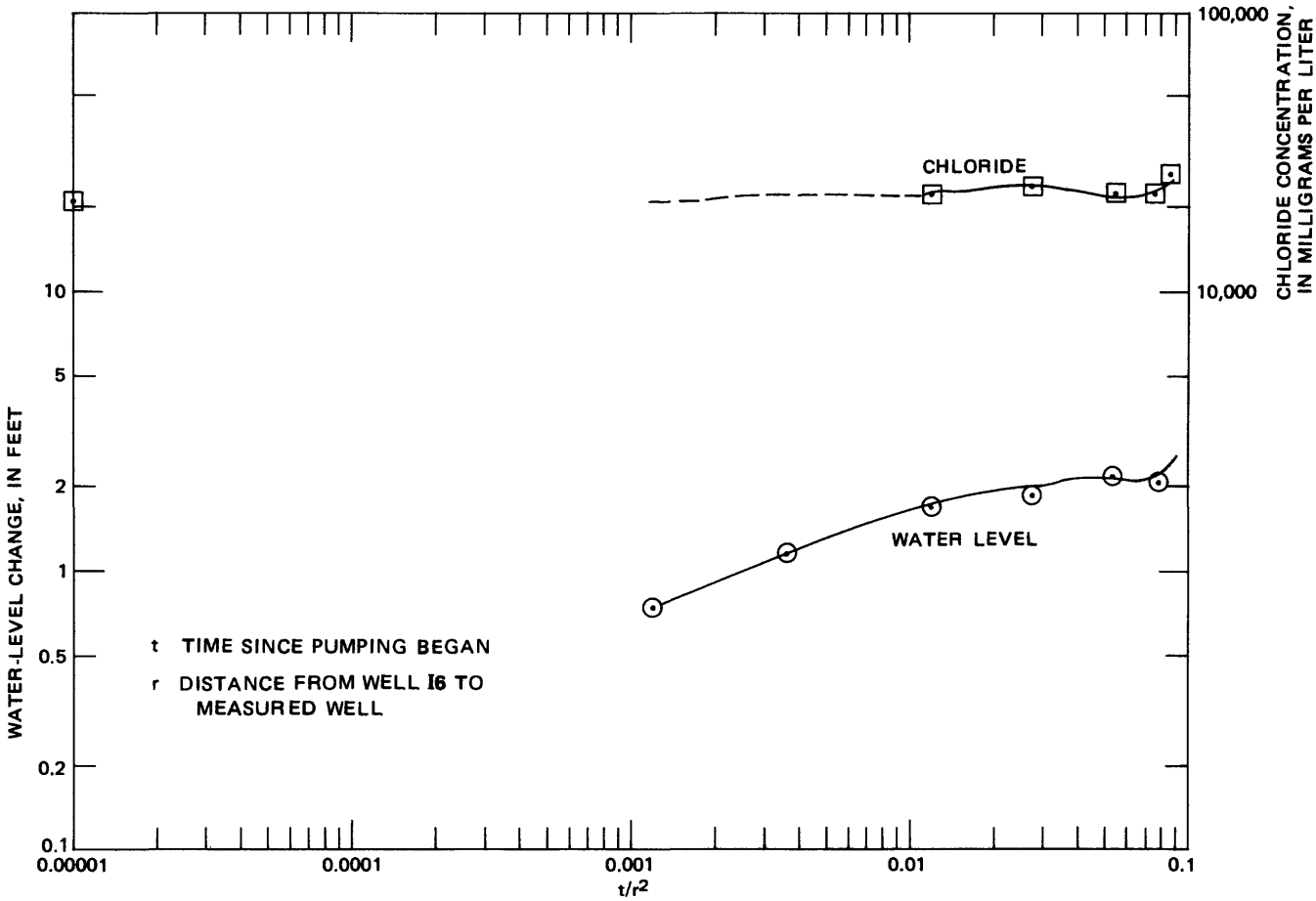

WATER-LEVEL AND CHLORIDE DATA AT WELL S16-DEEP

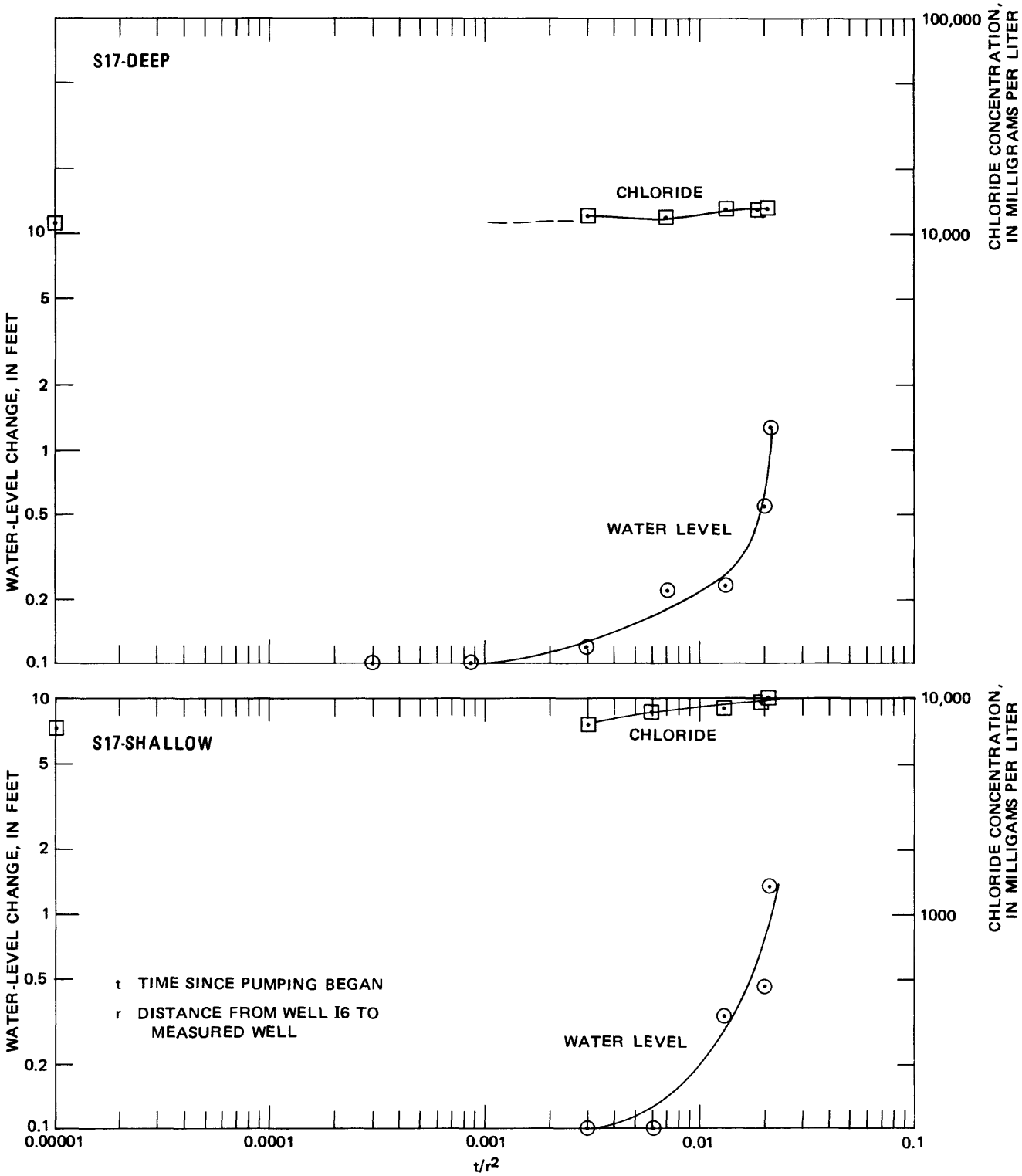

WATER-LEVEL AND CHLORIDE DATA AT WELL S17

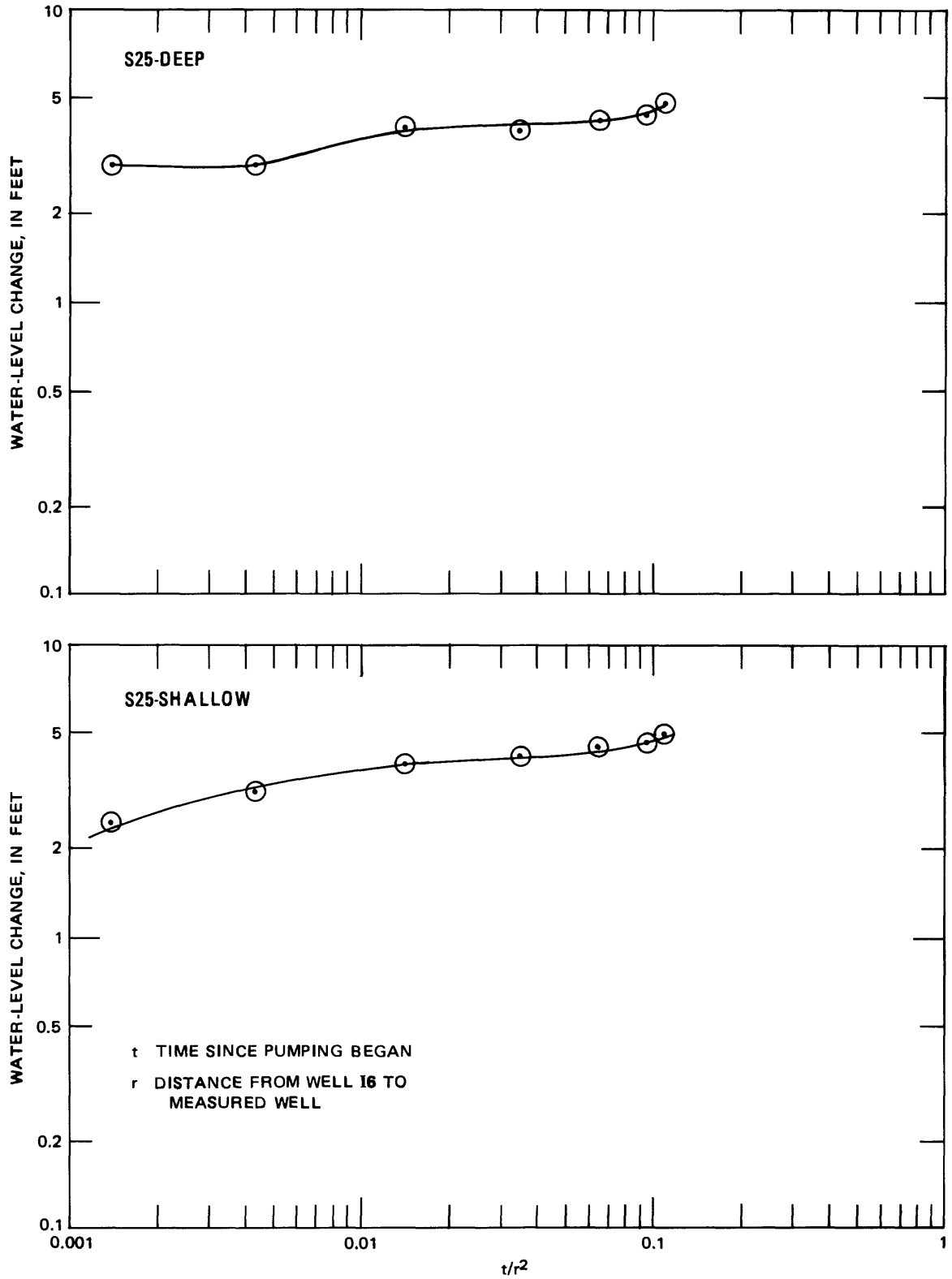

WATER-LEVEL DATA AT WELL S25

APPENDIX B.--Stable isotope ratios for hydrogen (δD) and oxygen ($\delta^{18}O$) and chloride concentration in surface and ground water

Sampling site	δD	$\delta^{18}O$	Chloride (mg/L)
Ground water			
U1	-52.5	-7.4	2,300
U3	-21.5	-2.0	30,000
U4	-22.5	-2.6	16,000
U5	-17.5	-2.0	26,000
U6	-23.0	-2.6	25,000
U7	-21.0	-2.2	28,000
U8	-22.0	-2.4	28,000
U9	-19.5	-2.1	30,000
U10	-19.0	-2.0	20,000
U11	-17.5	-2.0	31,000
U12	-17.5	-1.8	29,000
U13	-18.0	-1.5	31,000
U14	-18.0	-1.7	30,000
U15	-18.5	-1.7	31,000
U16	-20.5	-2.2	30,000
Surface water			
Mayfield Slough	-29.0	-3.6	--
Pond	-38.0	-4.6	--
Pond	-41.0	-5.0	--
Mayfield Slough	-51.5	-7.0	--
Matadero Creek	-53.5	-7.6	--
Matadero Creek	-55.5	-8.3	--

APPENDIX C.--Average pH and temperature at selected wells during 100-gal/min injection at well I6

Well	pH	Temperature (°C)
M2D	6.8	15.8
M2S	7.1	15.6
M3D	6.5	17.9
M3S	7.0	19.4
M4D	7.0	16.4
M4S	6.9	16.3
S10D	7.4	16.5
S12D	6.9	16.7
S12S	7.1	16.9
S13D	7.1	16.8
S13S	7.9	16.9
S15D	6.9	17.8
S16D	7.0	15.8
S17D	7.4	16.2
S17S	7.9	16.2
S25D	7.5	18.1
S25S	7.5	18.7